THE JOURNAL OF BIOLOGICAL CHEMISTRY VOL. 290, NO. 4, pp. 1898–1914, January 23, 2015

A Lettuce (*Lactuca sativa*) Homolog of Human Nogo-B Receptor Interacts with *cis*-Prenyltransferase and Is Necessary for Natural Rubber Biosynthesis*[S]

Received for publication, October 5, 2014, and in revised form, December 3, 2014 Published, JBC Papers in Press, December 4, 2014, DOI 10.1074/jbc.M114.616920

Yang Qu, Romit Chakrabarty, Hue T. Tran, Eun-Joo G. Kwon, Moonhyuk Kwon[1], Trinh-Don Nguyen, and Dae-Kyun Ro[2]

From the Department of Biological Sciences, University of Calgary, Calgary, Alberta T2N 1N4, Canada

Background: Natural rubber biosynthesis in lettuce (*Lactuca sativa*) and other plants remains elusive.
Results: An unusual *cis*-prenyltransferase-like protein interacts with and tethers a *cis*-prenyltransferase on endoplasmic reticulum, and its RNAi-silencing eliminates natural rubber.
Conclusion: *cis*-Prenyltransferase-like protein is a necessary component in natural rubber biosynthesis in lettuce.
Significance: The results presented here suggest hetero-protein complexes are involved in natural rubber biosynthesis.

Natural rubber (*cis*-1,4-polyisoprene) is an indispensable biopolymer used to manufacture diverse consumer products. Although a major source of natural rubber is the rubber tree (*Hevea brasiliensis*), lettuce (*Lactuca sativa*) is also known to synthesize natural rubber. Here, we report that an unusual *cis*-prenyltransferase-like 2 (*CPTL2*) that lacks the conserved motifs of conventional *cis*-prenyltransferase is required for natural rubber biosynthesis in lettuce. *CPTL2*, identified from the lettuce rubber particle proteome, displays homology to a human NogoB receptor and is predominantly expressed in latex. Multiple transgenic lettuces expressing *CPTL2-RNAi* constructs showed that a decrease of *CPTL2* transcripts (3–15% *CPTL2* expression relative to controls) coincided with the reduction of natural rubber as low as 5%. We also identified a conventional *cis*-prenyltransferase 3 (*CPT3*), exclusively expressed in latex. In subcellular localization studies using fluorescent proteins, cytosolic CPT3 was relocalized to endoplasmic reticulum by co-occurrence of CPTL2 in tobacco and yeast at the log phase. Furthermore, yeast two-hybrid data showed that CPTL2 and CPT3 interact. Yeast microsomes containing CPTL2/CPT3 showed enhanced synthesis of short *cis*-polyisoprenes, but natural rubber could not be synthesized *in vitro*. Intriguingly, a homologous pair CPTL1/CPT1, which displays ubiquitous expressions in lettuce, showed a potent dolichol biosynthetic activity *in vitro*. Taken together, our data suggest that CPTL2 is a scaffolding protein that tethers CPT3 on endoplasmic reticulum and is necessary for natural rubber biosynthesis *in planta*, but yeast-expressed CPTL2 and CPT3 alone could not synthesize high molecular weight natural rubber *in vitro*.

Natural rubber (NR)[3] is an important biopolymer used in the manufacture of hundreds of industrial products (1). NR displays exceptional physicochemical properties (*e.g.* elasticity and abrasion resistance) required for many heavy duty products. Despite progress in polymer chemistry, petroleum-derived synthetic rubber has not offered a comparable quality of rubber, making NR an indispensable raw material (2). Currently, the rubber tree (*Hevea brasiliensis*), primarily cultivated in tropical Asian countries, is almost the exclusive source of NR, but the supply of NR is not sustainable because of disease outbreak and unpredictable climate (3).

NR belongs to the isoprenoid class of natural products, which use isopentenyl diphosphate (IPP) as a central building block. IPP and its isomer dimethylallyl diphosphate undergo condensations to generate C10 geranyl diphosphate, C15 farnesyl diphosphate (FPP), and C20 geranyl geranyl diphosphate (4). In these reactions, dimethylallyl diphosphate serves as a primer on which IPPs are sequentially condensed in *trans*-configuration; thereby the enzymes catalyzing these reactions are referred to as *trans*-prenyltransferases (TPTs). On the other hand, in NR biosynthesis, a number of IPP molecules are conjugated onto a FPP molecule in *cis*-1,4-configuration by *cis*-prenyltransferase (CPT) (Fig. 1). Approximately 15,000 IPP molecules are condensed to form the NR polymer, with the weight average molecular weight (M_w) exceeding 1 million g/mol in rubber tree. The resulting NR biopolymer shows unique polymer features, including exclusive *cis*-configuration, extremely long polymer length, and narrow polydispersity (the spread of polymers). Although TPT and CPT share a similar mechanism involving a carbocation intermediate, they share no sequence homology (5). Crystal structures of TPT (FPP synthase) and CPT (undecaprenyl diphosphate synthase (UPPS)) further confirmed no structural similarity between these enzymes (5, 6) Thus, TPT

* This work was supported by funds from the Alberta Ingenuity New Faculty Award from Alberta Innovates Technology Future, the Natural Sciences and Engineering Research Council of Canada, and the Canada Research Chair (to D. K. R.).
[S] This article contains supplemental Tables S1 and S2.
[1] Supported by Next-Generation BioGreen 21 Program SSAC Grant PJ009549032014 from the Korean Rural Development Administration.
[2] To whom correspondence should be addressed: University of Calgary, Dept. of Biological Sciences, 2500 University Dr. NW, Calgary, AB T2N 1N4, Canada. Tel.: 403-220-7099; Fax: 430-289-9311; E-mail: daekyun.ro@ucalgary.ca.

[3] The abbreviations used are: NR, natural rubber; IPP, isopentenyl diphosphate; FPP, farnesyl diphosphate; TPT, *trans*-prenyltransferases; CPT, *cis*-prenyltransferase; UPPS, undecaprenyl diphosphate synthase; NgBR, Nogo-B receptor; qRT-PCR, quantitative real time PCR; RFP, red fluorescent protein; MRM, multiple reaction monitoring; GPC, gel permeation column; SRPP, small rubber particle protein; ER, endoplasmic reticulum; Y2H, yeast two-hybrid assay.

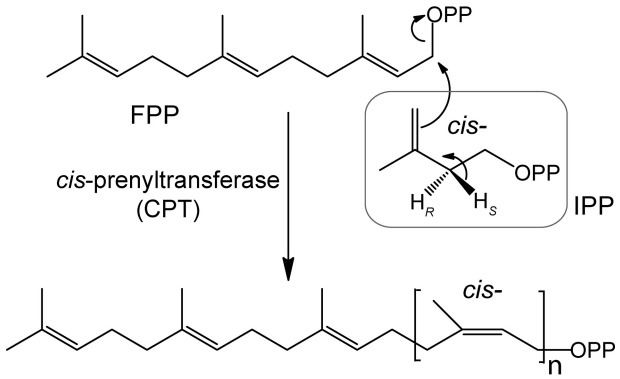

FIGURE 1. **Enzymatic synthesis of *cis*-polyisoprenes.**

and CPT are entirely different classes of enzyme and likely evolved independently.

In all living organisms, *cis*-isoprenoids with carbon length of C55 to C110 are ubiquitously present. Undecaprenyl diphosphate (C55) and dolichyl diphosphate (C70–C110) function as essential polysaccharide carrier molecules during cell wall biosynthesis in bacteria and *N*- and *O*-glycosylation of proteins in eukaryotes, respectively (7, 8). It was reported that *Escherichia coli* has a single *CPT* (*i.e.* UPPS), whereas yeast (*Saccharomyces cerevisiae*) has two *CPT*s, *RER2* and *SRT1*, responsible for C70–C110 dolichyl diphosphate biosynthesis (9–11). Null mutations of *E. coli UPPS* and double knock-out of the two yeast *CPT*s are lethal, confirming that they are essential genes (9, 11). In plants, studies of well annotated genomes showed that multiple copies of *CPT*s are present (12, 13), but the exact physiological role of each *CPT* is not fully understood.

NR is distinguishable from undecaprenol and dolichol in that it has significantly longer polymer length and is not involved in essential primary metabolism. It is important to note that 2,500 plant species can produce NR with M_w ranging from 10^5 to 2 million g/mol (14). Of particular interest is that several members of the Asteraceae family produce *cis*-polyisoprenes qualitatively comparable with the NR from rubber tree. For example, dandelion (*Taraxacum* spp.), lettuce (*Lactuca sativa*), and guayule (*Parthenium argentatum*) can synthesize NR of more than 1 million g/mol M_w (15–17). Although shorter than rubber tree NR, other Asteraceae plants, such as sunflower (*Helianthus* spp.) and goldenrod (*Solidago canadensis*), can also synthesize *cis*-polyisoprenes with M_w of $30–230 \times 10^3$ g/mol (17, 18). Therefore, studies of NR from these Asteraceae plants can help elucidate NR biosynthesis in plants.

At present, the molecular mechanism for NR biosynthesis, resulting in a wide range of M_w, remains elusive. NR from rubber tree is synthesized in the cytoplasm of laticifer cells (latex), a pipe-like tissue that develops alongside the phloem. Classical biochemical studies using latex have proposed a model where NR is synthesized on a monolayer organelle, known as the rubber particle, suspended in the latex (19). A rubber synthase complex is proposed to reside on the membrane of rubber particles with its catalytic domain exposed to the cytosol. In this model, the newly synthesized NR polymer extends into the core of the rubber particle using IPP substrates from the cytoplasm. However, molecular evidence for this model is scarce, and the rubber synthase mystery has remained unsolved for the past 50 years.

Considering the mechanistic commonality, it can be postulated that rubber synthases evolved from bacterial and eukaryotic *CPT*s. Recently, three dandelion *CPT*s displaying >96% amino acid identity were silenced by RNAi (20). The resulting transgenic dandelions showed elimination of NR in the latex, thereby proving the necessity of *CPT* in NR biosynthesis, although purified recombinant *CPT* activity was not reported. The *in vitro* synthesis of ~1 million g/mol NR was reported using *E. coli*-produced *H. brasiliensis* CPT co-incubated with latex fraction (21); however, yeast-produced *H. brasiliensis* CPT from the same clone only synthesized regular dolichol and not NR in comparable *in vitro* conditions (22), thereby questioning the *in vitro* NR synthetic activity of *H. brasiliensis* CPT. Currently, the *in vitro* synthesis of *cis*-polyisoprenes longer than undecaprenol and dolichol has not been achieved using purified recombinant CPT enzymes.

It was recently identified that the human Nogo-B receptor (NgBR) shares weak sequence homology to CPT (<15% at the amino acid level), and it lacks all five motifs conserved in all CPTs (23, 24). In humans, NgBR interacts with the Nogo-B peptide and Niemann-Pick type C2 (NPC2) protein to mediate signals for the proliferation of epithelial cells and to regulate intracellular cholesterol trafficking, respectively (23, 25). Interestingly, it also interacts with the human CPT enzyme (24). In plant, its homolog in *Arabidopsis* (*LEW1*) was identified during genetic screening for a leaf wilting phenotype (26). The *lew1* mutant is unable to efficiently synthesize dolichol, causing defects in *O*- and *N*-glycosylation of proteins. These results suggest that the CPT-like proteins have implications in dolichol biosynthesis in eukaryotes.

One difficulty of investigating rubber tree NR metabolism is that reverse genetic tools are not applicable to this perennial tropical tree. It was reported that an annual, transformable plant species, lettuce (*L. sativa*), could synthesize and store NR in rubber particles in the same manner as that of the rubber tree (15). In this work, we established lettuce as a model plant for the study of NR biosynthesis. Proteomic analysis identified a *CPT-like* (*CPTL*) gene as a homolog of NgBR, and its involvement in NR biosynthesis was comprehensively studied by reverse genetic, cell biological, and biochemical approaches. From these results, we conclude that *CPTL2* is necessary but not solely responsible for NR biosynthesis in lettuce.

EXPERIMENTAL PROCEDURES

Plant Material and Growth Condition—The seeds of *L. sativa* cv. Mariska and Ninja were obtained from the University of California Davis (Dr. Richard Michelmore). Lettuce plants were grown in a growth chamber at 20 °C and a 16-h photoperiod for 30 days. Plants were then transferred to 6-inch diameter pots and cultivated at the University of Calgary greenhouse at 23 ± 3 °C with a 16-h photoperiod.

RNA Isolation and Transcription Analysis—Fine powder (100 mg) ground in liquid nitrogen from various tissues or fresh latex (100 mg) was immediately mixed with 1 ml of TRIzol reagent (Invitrogen). RNA was isolated according to the manufacturer's protocol. First strand cDNA was synthesized

TABLE 1
A list of primers used in this work

	Primer name	Primer sequence
1	Gateway-Universal-F	GGGGACAAGTTTGTACAAAAAAGCAGGCTTC
2	Gateway-Universal-R	GGGGACCACTTTGTACAAGAAAGCTGGGTC
3	RNAi-a-F	AAAAAAGCAGGCTCTATGGATCTCGTAGG
4	RNAi-a-R	CAAGAAAGCTGGGTCACTATCCACCACAA
5	RNAi-b-F	AAAAAAGCAGGCTGATGAAGCTCGT
6	RNAi-b-R	CAAGAAAGCTGGGTAGGATCCTAAGTG
7	RNAi-c-F	AAAAAAGCAGGCTCAGCATGGCGTATTC
8	RNAi-c-R	CAAGAAAGCTGGGTAAAACACAGAGATTCTG
9	Gateway-CPTL2-R	CAAGAAAGCTGGGTCAGAACCGTAGTTCT
10	Gateway-CPTL2-TGA-R	CAAGAAAGCTGGGTCTTAAGAACCGTAGTTCT
11	Gateway-CPT3-F	AAAAAAGCAGGCTCTATGGAATTGGATCCAATCATTGC
12	Gateway-CPT3-R	CAAGAAAGCTGGGTCAGCCTGCTTCTTCTTCTTCTC
13	Gateway-CPT3-TGA-R	CAAGAAAGCTGGGTCTTAAGCCTGCTTCTTCTTCTTCTC
14	pUG23-CPTL2-F	GTTCACTAGTATGGATCTCGTAGGTGGA
15	pUG23-CPTL2-R	ACTCGTCGACAGAACCGTAGTTCTGCTTCACC
16	p415GPD-CPTL2-F	TAGAACTAGTGGATCCCCCAACATGGATCTCGTAGGTGGAC
17	p415GPD-CPTL2Flag-R	CGTCATCCTTGTAATCCCCAGAACCGTAGTTCTGCTTCA
17a	p415GPD-CPTL2N-R	CGAATTCCTGCAGCCCTTAAGAACCGTAGTTCTGCTTC
18	pUG23-synCPT3-F	GTTCACTAGTATGGAATTAGACCCTATCATCG
18a	p416GPD-synCPT3-F	TAGAACTAGTGGATCCCCCAACATGGAATTAGACCCTATCATCG
19	pUG23-synCPT3-R	GCCGGTCGACTGCTTGTTTCTTCTTCTTTTCATAG
19a	p416GPD-synCPT3Flag-R	CGTCATCCTTGTAATCCCCTGCTTGTTTCTTCTTCTTTTCATAG
19b	p416GPD-synCPT3N-R	CGAATTCCTGCAGCCCTCATGCTTGTTTCTTCTTCTTTTCA
20	p416GPD-RER2-F	CATAGACTAGTAACATGGAAACGGATAGTGGTATAC
21	p416GPD-RER2Flag-R	CGTCATCCTTGTAATCCCCATTCAACTTTTTTTCTTTCAAATCGAT
22	p416GPD-CPT1-F	TAGAACTAGTGGATCCCCCAACATGGATGTTAAAAAAAGAACACAAATCTAC
23	p416GPD-CPT1Flag-R	CGTCATCCTTGTAATCCCCTACATCGCTCCATATCTTCTTTTG
23a	p416GPD-CPT1N-R	CGAATTCCTGCAGCCCCTATACATCGCTCCATATCTTCTTT
24	pGAL-LexA-CPTL2-F	TAGCGGCCGCTTATGGATCTCGTAGGTGGA
25	PGAL-LexA-CPTL2-R	ACTCCTCGAGTTAAGAACCGTAGTTCTGCTTCACC
26	pJG4–6-CPTL2-F	GTTCCCATGGTTATGGATCTCGTAGGTGGA
27	pJG4–6-CPTL2-R	TAGCGGCCGCTTAAGAACCGTAGTTCTGCTTCACC
28	pGAL-LexA-SynCPT3-F	GTTCGCGGCCGCTCATGGAATTAGACCCTATCATCG
29	pGAL-LexA-SynCPT3-R	GCCGCTCGAGTTATGCTTGTTTCTTCTTCTTTTCATAG
30	pJG4–6-SynCPT3-F	GTTCGCGGCCGCATGGAATTAGACCCTATCATCG
31	pJG4–6-SynCPT3-R	GCCGGGATCCTTATGCTTGTTTCTTCTTCTTTTCATAG
32	Gateway-SRPP4-F	AAAAAAGCAGGCTCTATGGTGAGCAAGGGCGAGGAGC
33	Gateway-SRPP4-R	CAAGAAAGCTGGGTCTTATTCTTCCTGCACAGTTTCTCCCTCT
34	Gateway-Caleosin-F	AAAAAAGCAGGCTCTATGGCGACAGTGGCACCAATGGCA
35	Gateway-Caleosin-R	AAGAAAGCTGGGTCTTAATCCGTCTTTTTATTCGCTTTGGC
36	qPCR-Actin7-F	GGAGATGAGGCACAATCCAAAAGAGG
37	qPCR-Actin7-R	CACGGAGCTCGTTGTAGAAAGTGTGA
38	qPCR-CPT1-F	AAAGGCAATGGAGGCAACTGCTAA
39	qPCR-CPT1-R	TCTAGAACAGCATGGAAGATTTCATCGGT
40	qPCR-CPT2-F	TCGCCTTCTCATCTGACAACTGGT
41	qPCR-CPT2-R	ACTCGGATTTCGTCCCTCGACATA
42	qPCR-CPT3-F	GCTGAAACAAGCGGAAGACGAAAG
43	qPCR-CPT3-R	CTGGAATCGGGCGTGAAGAAATGA
44	qPCR-CPTL1-F	ATGAATGTGGCAGAGGATTTCCAACAGA
45	qPCR-CPTL1-R	CCCTAAGAATCAAGTGGAGAACATGCCATA
46	qPCR-CPTL2-F	GGCGTATTCGTTATACAGAGATGGTACAC
47	qPCR-CPTL2-R	AGAACCGTAGTTCTGCTTCACCTTG
48	p415GPD-CPTL1-F	TAGAACTAGTGGATCCCCCAACATGAATGTGGCAGAGGATTTC
49	p415GPD-CPTL1Flag-R	CGTCATCCTTGTAATCCCCTGAACCATAGTTTTGCTTGACC
50	p415GPD-CPTL1N-R	CGAATTCCTGCAGCCCTTATGAACCATAGTTTTGCTTGACC
51	pUG23-CPT1-F	TCGAGGATCCATGGATGTTAAAAAAAG
52	pUG23-CPT1-R	GCGTGTCGACTACATCGCTCCATATCTTCTTTTG
53	Flag-R	TTTCAAAGCTTGAATTCTCAGATCTTATCGTCGTCATCCTTGTAATCCCC

using SuperScript III reverse transcriptase (Invitrogen) and oligo(dT)$_{12-18}$ primer (Invitrogen) using 1–5 μg of total RNA. Quantitative real time PCR (qRT-PCR) was performed (Step One Real-Time PCR System; Applied Biosystems, Carlsbad, CA) using Power SYBER Green PCR Master Mix (Applied Biosystems), 5 μM primer, and cDNA template (equivalent to 5 ng of total RNA) in a reaction volume of 10 μl. The qRT-PCR program was 1 cycle of 95 °C for 10 min and 40 cycles of 95 °C for 15 s and 58 °C for 1 min. The critical threshold (Ct) values were used to calculate the relative transcript abundance using actin as the internal control as described (27). The primer efficiency was calculated from qRT-PCR of the serial dilution of total cDNA, and the specificity of the primers was confirmed by the dissociation curve for each primer set. The primers used for qRT-PCR are listed in Table 1 (primer numbers 36–47).

Isolation of Rubber Particles and Proteomics—Latex was collected as described (15) in ice-cold latex collection buffer. The samples were centrifuged at 10,000 × *g* for 2 min at 4 °C. The floating rubber layer was washed twice with latex collection buffer. The rubber particles were resuspended in latex storage buffer. The particle proteins were resolved on 10% SDS-PAGE. The gel was sliced into nine pieces. Trypsin digestion and subsequent LC-MS/MS analysis using MASCOT software (Matrix Science, Boston, MA) were carried out at the Southern Alberta Mass Spectrometry Center at the University of Calgary. Detailed methods were previously described (28). Reference

sequence file used for the MASCOT analysis was CLS_S3_ESTs_Sat.assembly (The Genome Center, University of California, Davis, CA).

Rubber Quantity and Quality Analysis—Fresh latex (50 mg) was mixed with 1 ml of acetone and centrifuged at 20,000 × *g* for 1 min. The pellet was allowed to dissolve in 1 ml of tetrahydrafuran overnight. The sample solution was filtered through a 0.45-μm polytetrafluoroethylene filter disk and subjected to HPLC (Waters Alliance HT 2795 separation module; Waters) analyses. Samples (50 μl) were injected and separated (mobile phase: 0.6 ml min^{-1} tetrahydrafuran) in tandem-connected GPCs with a linear separation range of 2×10^6 to 1×10^2 Da (Styragel HR 3 and Syragel HR 5; Waters) at 35 °C. The signal was detected by Waters 2420 ELS Detector (Waters) at 36 °C for nebulizer and 50 °C for drift tube. Empower2 chromatography Data Software (Waters) was used to analyze the data. Molecular mass and polydispersity were calculated based on *cis*-polyisoprene standards (Polymer Standards Service-USA, Amherst, MA). The relative rubber content was obtained from an external standard curve (ELSD peak area against a serial dilution of lettuce latex) and compared with that of the controls.

For visual rubber analysis in Fig. 5*A*, 350 mg (fresh weight) of latex was suspended in 1 ml of latex collection buffer and centrifuged at 10,000 × *g* for 5 min. For Fig. 5*B*, 30 mg of fresh weight of latex was suspended in 180 μl of 2% (w/v) SDS and centrifuged at 20,000 × *g* for 10 min at 4 °C.

CPT Transient Expression in Tobacco and Confocal Microscopy—The binary vectors for fluorescent protein tagging (pSITE-0B, -2NB, and -4NB with *CPT*/*CPTL*) were transformed into the *Agrobacterium* strain C58. Cells collected from an overnight culture were diluted in infiltration buffer (10 mM MES, pH 5.5, 10 mM $MgCl_2$, 150 μM acetosyringone) to A_{600} of 0.8 and incubated at room temperature for 2 h before infiltration into *Nicotiana benthamiana* leaves. The localization of CPTs was visualized after 2–4 days using a confocal microscope (Leica TCS SP5 II; Leica Microsystems Inc., Concord, Canada). The lipid substance was visualized by staining leaf samples with 0.5% (w/v) Nile Red in 70% ethanol for 20 min. The endoplasmic reticulum was visualized by co-infiltration with pBIN20-mCherry-HDEL. EGFP was detected by excitation at 488 nm and emission at 500–530 nm. RFP and mCherry were detected by excitation at 543 nm and emission at 590–650 nm. Nile red was detected by excitation at 543 nm and emission at 580–630 nm. Images from different excitations were sequentially collected.

Localization of CPT in Yeast—The vectors (pUG23 and p415GPD with *CPT/CPTL*) were transformed into a yeast strain EY0987 (ATCC 201389, MATα his3Δ1 leu2Δ0 lys2Δ0 ura3Δ0) with RFP-tagged ERG6 as a lipid body marker (29). An overnight culture was inoculated into fresh synthetic complete medium (1:100) containing 2% glucose and incubated at 30 °C. Localization of CPT/CPTL was determined at 8 h (log phase) and 20 h (stationary phase) after inoculation using a confocal microscope.

Yeast Two-hybrid Assay—The vectors (pGAL-LexA/pJG4-6 with *CPT/CPTL* and reporter plasmid pSH18-34 for β-galactosidase) were transformed into a yeast strain JC1280 (MATα; his3 trp1 ura3-52 leu2::proLEU2-lexAop6) (30). Multiple colonies were inoculated in 2 ml of synthetic complete medium containing 2% raffinose. Cells (0.5 ml) from an overnight culture were inoculated into 2 ml of synthetic complete medium containing either 2% glucose or 2% galactose and incubated at 30 °C for 6 h. Yeast cells, equivalent to 1 ml of culture with A_{600} between 0.6 and 1.0, were collected and resuspended in 1 ml of Z buffer (60 mM Na_2HPO_4, 40 mM NaH_2PO_4, 10 mM KCl, 1 mM $MgSO_4$, 50 mM β-mercaptoethanol, pH 7), followed by lysis by vortexing for 20 s with the addition of 20 μl of chloroform and 20 μl of 0.1% SDS. The mixture was incubated at 28 °C for 5 min. The reaction was started by addition of 0.2 ml of 4 mg ml^{-1} orthonitrophenyl-β-galactoside in Z-buffer and was stopped by addition of 0.5 ml of 1 M Na_2CO_3 after 2.5–5 min. The mixture was centrifuged at 20,000 × *g* for 5 min, and the A_{420} of the supernatant was read. The β-galactosidase activity was calculated in Miller units.

Generation of DNA Constructs—The primer sequences are listed in Table 1. Three RNAi fragments of *CPTL2* cDNA were sequentially amplified by primers (primers 3/4, 5/6, and 7/8) and universal Gateway cloning primers (1/2). The amplicons were cloned into an RNAi binary vector pK7GWIWG2D[II] (Plant Systems Biology, VIB-Ghent University, Belgium), sequentially using the Gateway BP Clonase and Gateway LR Clonase (Invitrogen). For GFP tagging and overexpression in plant, full-length *CPTL2* was amplified with primers 3/9 and 3/10 and cloned into binary vector pSITE-2NB and pSITE-0B, respectively (31). For GFP and RFP tagging, full-length *CPT3* was amplified with primers 11/12 and cloned into pSITE-2NB and pSITE-4NB vectors, respectively. For expression of GFP-tagged, FLAG-tagged, and nontagged CPTL2 in yeast, *CPTL2* was amplified from lettuce latex cDNA with primer 14/15 for GFP tagging, first PCR with primer 16/17 and second PCR with primer 16/53 using the first PCR product as template for FLAG tagging, primer 16/17a for nontagged version), and cloned into pUG23 for GFP-tagging and in p415GPD for both FLAG-tagged and nontagged versions. *CPTL1* was also similarly cloned into p415GPD using primers (first PCR with 48/49 and second PCR with 48/53 using the first PCR product as template for FLAG-tagging and 48/50 for nontagged version). The synthetic *CPT3* (synCPT3; Genscript, Piscataway, NJ), optimized for codon usage in yeast, was cloned into pUG23 for GFP tagging using primers 18/19 and into p416GPD for both FLAG- and nontagged versions using primers (first PCR with 18a/19a and second PCR with 18a/53 using the first PCR product as template for FLAG-tagging and 18a/19b for nontagged version). Similarly, *CPT1* was amplified from lettuce latex cDNA with primers (51/52 for GFP-tagging, first PCR with 22/23 and second PCR with 22/53 using the first PCR product as template for FLAG-tagging and 22/23a for nontagged version) and cloned into pUG23 for GFP-tagging and in p416GPD for both FLAG-tagged and nontagged versions. The yeast RER2 was amplified from yeast genomic DNA and cloned into p416GPD for FLAG tagging with primers (first PCR with 20/21 and second PCR with 20/51 using the first PCR product as template). For the yeast two-hybrid assay (Y2H), *CPTL2* and *synCPT3* were cloned into pGAL-LexA and pJG4-6 vectors with primers 24/25, 28/29, 26/27, and 30/31, respectively. For expres-

sion in *E. coli*, *CPTL2* and *synCPT3* were cloned into the pDONOR221/pDEST17 vector (Invitrogen) using primers 3/10 and 11/13, respectively. Recombinant Small rubber particle protein 4 (SRPP4) and Caleosin were cloned into pDONOR221/pDEST17 using primers 32/33 and 34/35, respectively.

Agrobacterium-mediated Plant Transformation—Leaf explants for transformation were obtained from seedlings (1–2 months old), cultivated at 25 °C with a 16-h photoperiod and 45% relative humidity in Murashige and Skoog medium. Overnight culture of *Agrobacterium tumefaciens* strain LBA4404 carrying the specific binary plasmid was used to infect the leaf explants and thereafter co-cultivated in Murashige and Skoog medium supplemented with 0.2 mg liter^{-1} 6-benzylaminopurine (Sigma-Aldrich) and 0.2 mg liter^{-1} 1-naphalene acetic acid (Sigma-Aldrich) for 2 days at 25 °C with a 16-h day/8-h night photoperiod and 45% relative humidity (the growth condition remained the same unless specified). Subsequently, the explants were transferred to Murashige and Skoog medium supplemented with 0.2 mg liter^{-1} 6-benzylaminopurine, 0.2 mg liter^{-1} 1-naphalene acetic acid, 25 mg liter^{-1} kanamycin (Amresco, Solon, OH), and 250 mg liter^{-1} cefotaxime (Duchefa Biochemie, Haarlem, Netherlands). The putative shoots were placed in rooting medium containing 0.1 mg liter^{-1} 1-naphalene acetic acid, 12.5 mg liter^{-1} kanamycin, and 250 mg liter^{-1} cefotaxime. After rooting, the shoots were screened for GFP expression through confocal microscopy, transferred to potted soil in growth chamber (for 1 month), and then transferred to the greenhouse for further growth and analyses.

CPT and CPTL Expression in E. coli—For CPTL2, *E. coli* BL21-AI cells (Invitrogen) with GST-CPTL2 in pGEX-6p-2 vector (GE Healthcare Life Sciences) were cultured at 37 °C in 1 liter of LB medium until an A_{600} of 0.5 was reached, and then cells were induced with 0.1% arabinose and 0.4 mM isopropyl β-D-thiogalactopyranoside. Cells were grown at 15 °C for 24 h. The cells were collected and resuspended in lysis buffer (25 mM Tris-HCl, pH 7.5, 100 mM NaCl, 10% (v/v) glycerol, 1 mM PMSF). After sonication, the soluble fraction was incubated for 1 h with 1 ml of pre-equilibrated glutathione resin. The column was washed with wash buffer (50 mM Tris-HCl, pH 8, 100 mM NaCl, 1 mM EDTA, 1 mM DTT, 0.1% (v/v) Triton X-100) and eluted with elution buffer (50 mM Tris-HCl, pH 8, 100 mM NaCl, 1 mM EDTA, 1 mM DTT, 10 mM reduced glutathione). For CPT3, *E. coli* BL21AI cells with His_6-CPT3 in pDEST17 vector were cultured at 37 °C in 0.3 liter of LB medium until an A_{600} of 0.6 was reached and then induced with 0.2% arabinose at 37 °C for 0.5 h. The cells were collected and resuspended in lysis buffer (25 mM Tris-HCl, pH 7.5, 100 mM NaCl, 10% (v/v) glycerol, 1 mM PMSF, 1 mM DTT). After sonication, the soluble fraction was incubated for 1 h with 1 ml of nickel-nitrilotriacetic acid resin. The column was washed with 30 ml of wash buffer (25 mM Tris-HCl, pH 7.5, 100 mM NaCl, 10% (v/v) glycerol, 1 mM PMSF, 0.01% (v/v) Triton X-100, and 25 mM imidazole) and was eluted with elution buffer (25 mM Tris-HCl, pH 7.5, 100 mM NaCl, 10% (v/v) glycerol, 1 mM PMSF, and 500 mM imidazole).

CPT Expression in Yeast and Microsome Isolation—The p415GPD or p416GPD vector containing *CTPL1/2* or *CPT1/3*, respectively, either with C-terminal FLAG or without any tagging was transformed into YPH499 yeast strain using a standard lithium acetate transformation protocol. Transformed yeast cells were grown to mid-late logarithmic phase in synthetic complete medium with glucose lacking uracil and leucine. The cell pellet was broken open by glass bead-beating method (Bio-Spec Products) in TES-B buffer (50 mM Tris-HCl, pH 7.4, 1 mM EDTA, 500 mM D-sorbitol). For microsome preparation, the cell lysate was centrifuged at 10,000 × *g* for 10 min at 4 °C. The supernatant was further centrifuged at 100,000 × *g* for 1 h at 4 °C. The microsome pellet was resuspended in TG buffer (50 mM Tris-HCl, pH 7.4, 20% (v/v) glycerol) and stored at −80 °C.

Immunoblot Analysis—Yeast microsomal protein or total protein was separated by SDS-PAGE on 12% SDS-PAGE and transferred to PVDF membrane. The membrane was hybridized with 1:2000 diluted anti-FLAG antibody (Sigma-Aldrich) and 1:5000 diluted anti-mouse secondary antibody (sheep anti-mouse; GE Healthcare Biosciences), developed with Amersham Biosciences ECL Plus Western blotting detection reagent (GE Healthcare Life Sciences), and exposed to a film. For DPM1 detection, 1:1000 diluted anti-DPM1 antibody (Life Technologies) and 1:10,000 diluted anti-mouse secondary antibody were applied to the same blot after stripping.

CPT Enzyme Assay and TLC—Yeast microsomes (50 μg of protein) containing recombinant CPT/CPTL was assayed as described (24). The 50-μl reaction mixture contained: 50 μM FPP (Echelon, Biosciences Inc., Salt Lake City, UT), 175 μM IPP (Echelon, Biosciences Inc., Salt Lake City, UT), 25 μM ^{14}C-IPP (1.1 × 105 dpm; PerkinElmer Life Sciences), 50 mM HEPES, pH 7.5, 5 mM $MgCl_2$, 2 mM DTT, 2 mM Na_3VO_4, and 2 mM NaF. The reaction was incubated at 30 °C for 2 h and then extracted with 1 ml of chloroform:methanol (2:1 v/v) and 0.4 ml of 0.9% (w/v) NaCl. After partitioning by centrifugation, the chloroform fraction was washed three times with 0.5 ml of chloroform:methanol:water (3:48:47 v/v/v), and a 10% aliquot was assayed for radioactivity by scintillation counting. The remaining extraction was dried down completely and hydrolyzed in 1 M HCl for dephosphorylation by incubating at 85 °C for 1 h, followed by equal volume extraction twice with benzene. Benzene was dried down to a small volume for spotting on TLC plate. C18 reverse silica plate (Whatman) was used for separation in acetone:water (39:1 v/v) solvent. The TLC plate was exposed to a phosphorimaging screen (GE Healthcare) for the indicated number of days before scanning in Molecular Imager FX (Bio-Rad).

Multiple Reaction Monitoring—SRPP4 and caleosin were used as the internal calibrators for CPTL2 and CPT3 quantitation. Full-length SRPP4 and calsosin were amplified with primers 32/33 and 34/35, respectively (Table 1) and extended with primers 1/2. Both genes were cloned with Gateway cloning into pDEST17 vector (Invitrogen), according to the manufacturer's protocol. The vectors were transformed to BL21-AI cells (Invitrogen). The cells were cultured at 37 °C in 2 ml of LB medium until an A_{600} of 0.6 was reached and then were induced with 0.2% arabinose at 37 °C for 0.5 h. The cells were collected and resuspended in lysis buffer (25 mM Tris-HCl pH 7.5, 100 mM

NaCl, 10% (v/v) glycerol, 1 mM PMSF, 1 mM DTT). After sonication, the total pellets were collected, resuspended in lysis buffer, and resolved in 12% SDS-PAGE. The recombinant protein bands were cut from the gel and subjected to multiple reaction monitoring (MRM). Multiple reaction monitoring by LC-MS/MS was performed by UC Davis Proteomics Core Facility. Peptides and daughter ions used were shown in supplemental Table S2. For in-gel digestion, gel pieces were cut into ~1-mm cubes and washed two times with 50 mM ammonium bicarbonate, pH 8, and then dehydrated with 100% acetonitrile. The gel pieces were reduced with 10 mM dithiothreitol for 30 min at 56 °C. The gel pieces were then dehydrated with 100% acetonitrile and alkylated with 55 mM iodoacetamide for 20 min. The gels were then washed with 50 mM ammonium bicarbonate, dehydrated one last time, and digested overnight at 37 °C using modified sequencing-grade trypsin (Promega Bio-Sciences). For extraction, the supernatant was collected and put into a fresh tube. Next, 60% acetonitrile:0.1% trifluoroacetic acid was added to the gel pieces, sonicated for 10 min, and centrifuged for 8 min. The supernatant was then removed and added to the fresh tube. The supernatant was then vacuum-centrifuged until dry.

Peptides from candidate proteins were selected based on prior shotgun LC-MS/MS data. All peptides were selected based on the following criteria: uniqueness to the targeted protein; fully tryptic (*i.e.* no missed cleavages or ragged ends); and absence of potentially modified amino acids. Cysteine-containing peptides were presented as carbamidomethylated derivatives. Acquisition scheduling was performed using the Skyline Retention Time (iRT) predictor calculator. A heavy peptide retention time calibration mixture (Thermo Scientific) was spiked into each LC-MRM-MS run to monitor for retention time shift. LC-MRM-MS analysis was performed on a TSQ Vantage Triple Quadrupole mass spectrometer (Thermo-Fisher Scientific) in conjunction with an Advance Splitless Nano UHPLC and an Advance Autosampler (Bruker-Michrom, Auburn, CA). 10 μl of the digested peptides and 1 μl of the retention time mixture were loaded onto a Michrom C18 trap and desalted before they were separated using a Michrom 200 μm × 150 mm Magic C18AQ reverse phase column. A flow rate of 2 μl min^{-1} was used. Peptides were eluted using a 60-min gradient with 5% B to 35% B for 50 min, 35% B to 80% B for 1 min, 80% B for 1 min, 80% B to 5% B for 1 min, and finally held at 5% B for 7 min (A = 0.1% formic acid, B = 100% acetonitrile). The mass spectrometer was operated with a spray voltage of 1.8 kV, a capillary temperature of 200 °C, and a normalized collision of 35%. Peak areas for each peptide were extracted and integrated using Skyline v1.4.

Nucleotide Sequence Deposition—The nucleotide sequences of the cDNAs reported in this paper have been submitted to GenBank™ with the following accession numbers: CPTL1, KF752484; CPTL2, KF752485; CPT1, KF752486; CPT2, KF752487; and CPT3, KF752488.

RESULTS

Identification of a Distinct CPT from Lettuce—NR with M_w of 1.27 million g/mol and polydispersity value of 1.1 was previously reported from *L. sativa*, cv. Salinas (15). Using an HPLC gel permeation column (GPC), these literature data were corroborated in two different lettuce cultivars, Mariska and Ninja. The M_w and polydispersity from Mariska and Ninja were comparable to each other and slightly higher than the reported values in Salinas (Table 2). Because NR accumulates in the stem, early bolting and flowering facilitate NR studies in lettuce. Mariska was used initially in this study. However, because Ninja flowers ~50 days earlier than Mariska, Ninja was primarily used to expedite the research progress.

TABLE 2
Weight average molecular weight (M_w) and polydispersity of NR from *L. sativa* cv. Mariska and Ninja

	L. sativa cv. Mariska	*L. sativa* cv. Ninja
M_w (million g/mol)[a]	1.50 ± 0.07	1.45 ± 0.03
Polydispersity[a]	1.53 ± 0.06	1.49 ± 0.10
Flowering time[b]	135 ± 4	84 ± 9

[a] The values are the means ± S.D. from three individual plants.
[b] The values indicate the number of days from germination to the first flowering (means ± S.D.; Mariska, n = 14; Ninja, n = 15).

Lettuce (cv. Mariska) liquid latex samples were centrifuged and separated into three fractions: floating rubber particles, soluble fraction, and precipitated bottom fraction. The floating rubber particle layer was collected and fractionated on SDS-PAGE, and the protein gel containing proteins from 10 to ~400 kDa was divided into nine pieces. Each section was subjected to LC-MS/MS-based protein identification using MASCOT software to interrogate a reference lettuce transcriptome comprised of 29,417 unigenes. As a result, 372 unigenes were identified by at least two peptides with $p < 0.05$ or 1 peptide with $p < 0.01$. The proteins identified from the lettuce rubber particles are listed in supplemental Table S1.

SRPP homologs, previously shown to be localized on rubber particles, were among the proteins identified; however, *cis*-prenyltransferase (*CPT*) was not initially identified. Upon careful examination, two lettuce unigenes were identified, which were annotated as homologs of *Lew1* in *Arabidopsis* and Nogo-B receptor (*NgBR*) in human. Both genes have been implicated in dolichol metabolism (24, 26).

Sequence analysis of these two lettuce unigenes revealed that both are transcribed from the same gene, and the full-length cDNA, encoding a polypeptide of 244 amino acids, was isolated from lettuce cv. Mariska. Because of its low sequence homology to the conventional *CPT* sequences, this newly identified lettuce cDNA was named *CPT-Like2* (*CPTL2*). One additional homolog, displaying 68.9% amino acid identity to *CPTL2*, was also identified from the lettuce transcript database and was named *CPTL1*. The deduced protein sequences from the *CPTL1/2* cDNAs show ~45 and ~25% identity to Lew1 and NgBR, respectively.

As the focus of this work is NR biosynthesis in plants, *CPTL* homologs were also searched and identified from the rubber tree and dandelion. The rubber tree has one *CPTL*, whereas the dandelion has two *CPTLs* in the public database. To gain a better insight into the CPTL sequences, the protein sequences of these CPTLs were aligned with other CPTs including the CPTs from *E. coli* and yeast (Fig. 2). The three-dimensional crystal structure and site-directed mutagenesis of the prokaryotic CPTs have revealed five conserved motifs, most of which

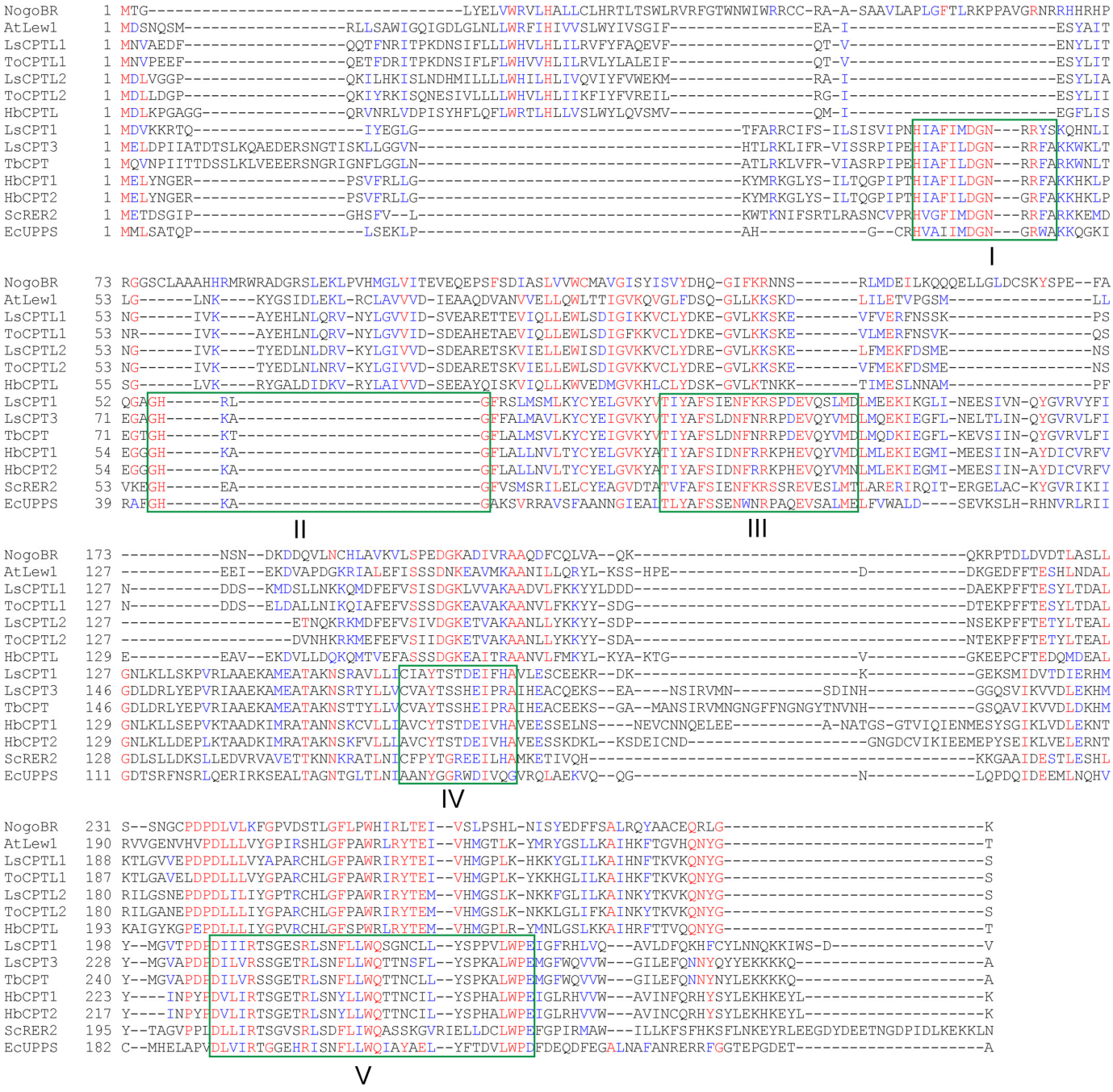

FIGURE 2. **A sequence alignment of various CPT and CPTL proteins.** *Green boxes* are the amino acids conserved in CPTs. Detailed information can be found in Refs. 32 and 33. *To*, *Taraxacum officinalis*; *Hb*, *H. brasiliensis*; *Ec*, *Escherichia coli*; *Sc*, *S. cerevisiae*; *Ls*, *L. sativa*; *Tb*, *T. brevicorniculatum*. The GenBank accession numbers are: NgBR (BC150654), AtLew1 (At1G11755), HbCPTL (JT945746), ToCPTL1 (DY820019), ToCPTL2 (DY832694), TbCPT (JQ991925), HbCPT1 (AB061234), HbCPT2 (AB064661), EcUPPS (EU906097), and ScRER2 (AB013497).

are involved in substrate-binding, catalysis, or structural interactions (32, 33 and references therein). Although weak sequence similarities between CPTLs and CPTs were found, none of the five motifs of CPTs was conserved in the CPTLs (Fig. 2), implying that CPTLs are not likely to have the catalytic functions found in the conventional CPTs.

Latex-specific Expression of CPTL2—The relative transcript abundance of *CPTL2* was examined in different lettuce tissues, including latex isolated from three different developmental stages of lettuce by qRT-PCR. For comparison, two conventional *CPT*s (*CPT1/2*) possessing conserved catalytic motifs were also identified from the lettuce transcript database and included in the qRT-PCR analysis. *CPTL2* was exclusively expressed in latex with the highest expression in the latex of the flowering stage (up to 32-fold higher in latex relative to leaves; Fig. 3*A*). This latex-specific expression was not observed for its closest homolog, *CPTL1*, and two other *CPT* genes (*CPT1* and *CPT2*). *CPTL1* and *CPT1* displayed ubiquitous expression in all tissues, whereas *CPT2* showed a higher level of expression in green leaves than other tissues. This qRT-PCR result suggests the possible involvement of *CPTL2* in NR biosynthesis in lettuce.

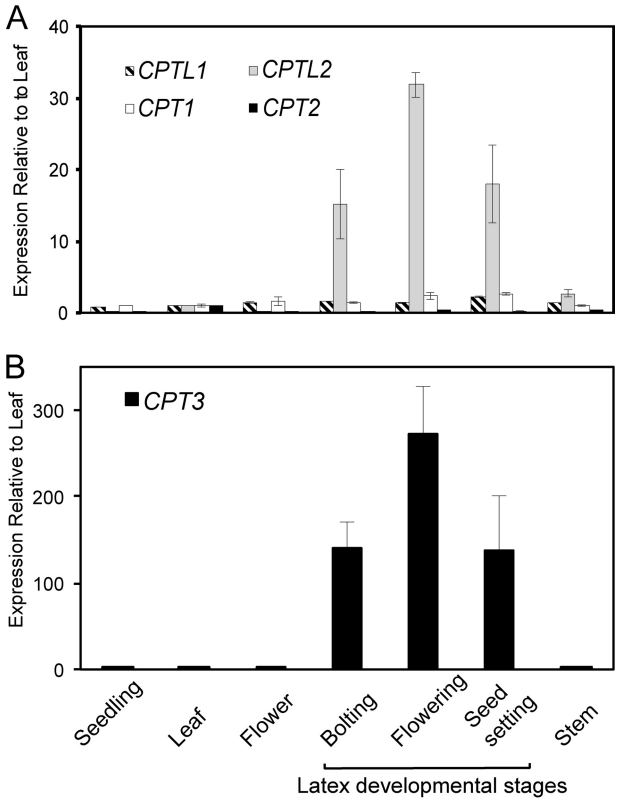

FIGURE 3. **Relative quantitation of *CPT* and *CPTL* transcripts in lettuce.** *A*, relative *CPT1/2* and *CPTL1/2* transcripts from various lettuce (cv. Mariska) tissues were measured by qRT-PCR, relative to the respective transcripts in leaf (first true leaf). *B*, relative *CPT3* transcript levels were measured in the same tissues as in *A*, relative to the leaf transcript level (cv. Mariska). The data are means ± S.D. from three biological replicates, each including three technical replicates. Actin was used to normalize the data.

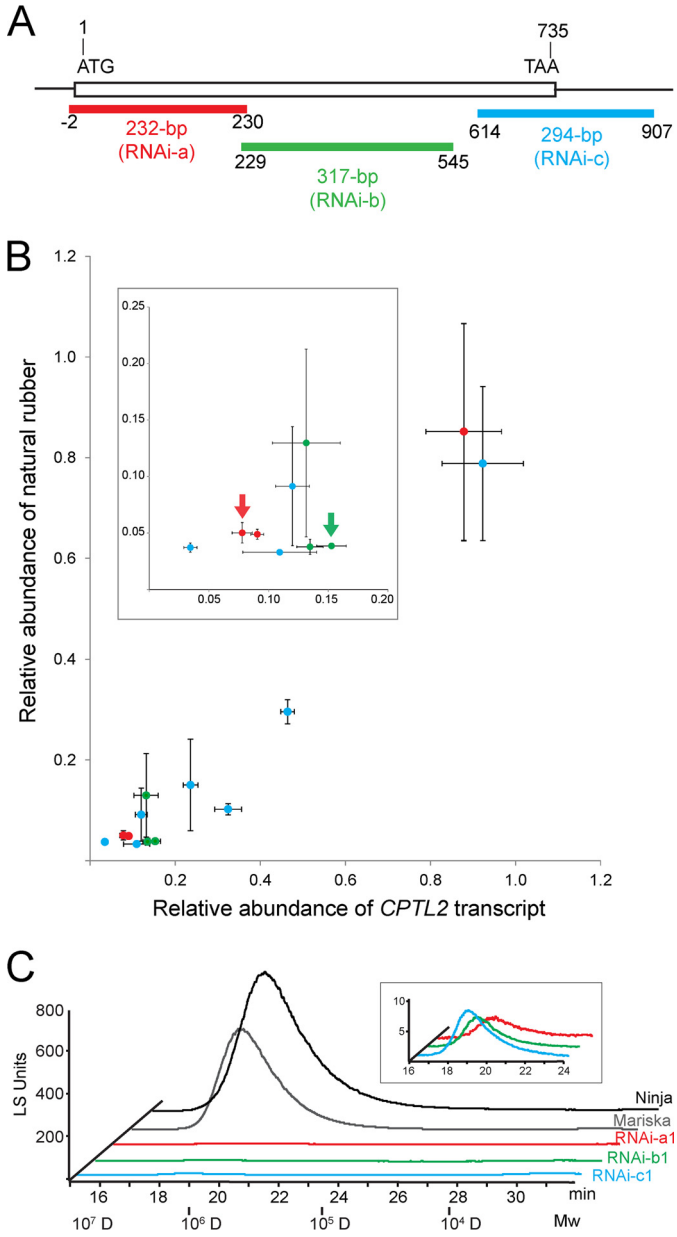

FIGURE 4. **Experimental design and characterization of *CPTL2*-silenced lettuce.** *A*, the positions of the different RNAi-silencing constructs (RNAi-a, -b, and -c) in the *CPTL2* are shown and color-coded. *B*, relative abundance of the *CPTL2* transcript is plotted against relative NR abundance from 13 independent transgenic lettuces. Data points in *red*, *green*, and *blue* are from RNAi-a, -b, and -c constructs, respectively. Each value is calculated from three independent T2 plants derived from an independent T1 transgenic line. NR abundances are from three biological replicates, and relative transcripts are from three biological replicates, each including three technical replicates. Two transgenic lettuces designated by *red* and *green arrows* were subjected to the relative CPTL2 protein quantification by multiple reaction monitoring. Numerical data and lettuce cultivars are given in Table 3. *C*, chromatographic separation of the NR by HPLC-GPC. Wild-type lettuces (Ninja and Mariska) were used as controls.

Silencing of CPTL2 in Lettuce Causes a Decrease in NR—Next, we examined the function of *CPTL2* using RNAi in lettuce. Three independent *CPTL2-RNAi* constructs driven by the cauliflower mosaic virus 35S promoter were designed from different regions of the *CPTL2* transcript (denoted as RNAi-a, -b, and -c; Fig. 4*A*). The use of three independent constructs in the silencing experiments reduces the occurrence of false positives arising from off-target effects. A total of 13 transgenic lettuce lines were established using Mariska (for RNAi-a) and Ninja (RNAi-b and RNAi-c) cultivars. For all 13 transgenic lines, three individual T2 plants from an independent T1 transgenic line were used to measure the relative abundance of NR and *CPTL2* transcripts. Nontransformed lettuce, vector-transformed lettuce, and wild-type segregant from the T2 generation were used as control plants. Of these, six transgenic lettuces (RNAi-a1, -a3, -b1, -b3, -c2, and -c4) derived from three distinct *CPTL2*-RNAi constructs showed less than 5% of NR in comparison with controls (Fig. 4*B* and Table 3 in bold characters). The relative *CPTL2* transcript levels of these six lines were reduced accordingly to 3–15%. Conversely, two transgenic lines without NR reduction (RNAi-a2 and -c8) did not show any corresponding reduction of *CPTL2* transcripts. Overall, the NR abundance and *CPTL2* transcripts in 13 transgenic lettuces showed a strong linear correlation (Fig. 4*B*).

To further confirm that a decrease in *CPTL2* transcript also reduces CPTL2 protein levels in transgenic lettuce, CPTL2 antibodies were generated; however, the antibodies produced were not suitable for latex immunoblot assays because of cross-reactivity. Therefore, CPTL2 proteins from two independent transgenic lettuces (RNAi-a1 and RNAi-b1) were quantified by MRM using LC-MS/MS. Latex caleosin (25.5 kDa) and small rubber particle protein 4 (SRPP4, 25.4 kDa), both of which migrate closely with CPTL2 (28.4 kDa), were used as internal

TABLE 3

Weight average molecular weight (M_w) and polydispersity (Pd) of *cis*-polyisoprene from *CPTL2*-silenced lettuce

Bold type indicates transgenic lettuces derived from three distinct *CPTL2*-RNAi constructs that showed less than 5% of NR in comparison with controls.

Plant	M_w[a]	Pd[a]	Relative abundance of *cis*-polyisoprene[a]
	million g/mol		
Mariska control[b]	1.29 ± 0.04	1.22 ± 0.04	1.00 ± 0.12
CPTL2-a1	1.20 ± 0.09	1.31 ± 0.03	**0.05 ± 0.01**
CPTL2-a2	1.28 ± 0.05	1.50 ± 0.02	0.85 ± 0.22
CPTL2-a3	1.15 ± 0.07	1.32 ± 0.08	**0.05 ± 0.01**
Ninja control[b]	1.37 ± 0.05	1.42 ± 0.02	1.00 ± 0.25
CPTL2-b1	1.39 ± 0.06	1.22 ± 0.04	**0.04 ± 0.01**
CPTL2-b2	1.36 ± 0.12	1.39 ± 0.07	0.13 ± 0.08
CPTL2-b3	1.32 ± 0.06	1.29 ± 0.12	**0.04 ± 0.01**
CPTL2-c1	1.13 ± 0.15	1.43 ± 0.05	0.09 ± 0.05
CPTL2-c2	1.28 ± 0.08	1.32 ± 0.13	**0.04 ± 0.01**
CPTL2-c3	1.25 ± 0.04	1.40 ± 0.04	0.10 ± 0.02
CPTL2-c4	1.26 ± 0.02	1.44 ± 0.03	**0.03 ± 0.01**
CPTL2-c5	1.31 ± 0.04	1.37 ± 0.07	0.15 ± 0.09
CPTL2-c7	1.24 ± 0.06	1.43 ± 0.01	0.29 ± 0.04
CPTL2-c8	1.24 ± 0.06	1.44 ± 0.01	0.77 ± 0.14

[a] The values of the RNAi lines are means ± S.D. ($n = 3$) and were measured from three T2 transgenic plants derived from independent T1 transgenic lines.
[b] The data for controls were generated from two of nontransformed lettuce (Mariska for CPTL2-a line or Ninja for CPTL2-b/c lines), two of vector-transformed lettuce, and two of wild-type segregants from the T2 population ($n = 6$).

calibration proteins. Prior to the experiment, recombinant CPTL2, caleosin, and SRPP4 proteins were generated and used to select the most suitable peptides for MRM. The optimized MRM method was then used to calculate the relative quantity of CPTL2 in reference to caleosin and SRPP4 in latex. The relative CPTL2 protein abundance in the RNAi-a1 and RNAi-b1 lettuce lines were determined to be 19.2 and 18.3% of the controls, respectively (*two arrows* in Fig. 4*B* and supplemental Table S2). Therefore, significant decreases of *CPTL2* transcript, CPTL2 protein, and NR were observed in the transgenic plants. Although NR was markedly decreased in transgenic lettuces, the M_w and polydispersity values of NR from *CPTL2*-silenced lettuce were not different from those of the controls (Table 3). Therefore, we concluded that the silencing of *CPTL2* in lettuce results in marked reduction of NR in latex without altering the NR polymer properties.

The chemical phenotype of latex from transgenic plants was apparent in GPC chromatographic separation (Fig. 4*C*). However, the reduction of the floating rubber particles using a centrifugal method was only noticeable upon close observation (Fig. 5*A*). The thickness and dry weight of the rubber particle layers from the *CPTL2*-silenced lettuce were ~60% of those from the controls. We reasoned that the dramatic decrease of NR from *CPTL2*-silenced lettuce should be observable in latex. Therefore, we attempted to develop a simple method to sufficiently visualize the NR deficiency in latex. It was found that the addition of an appropriate amount of sodium dodecyl sulfate to latex allows the formation of optically dense NR colloids in NR-rich controls after centrifugation (Fig. 5*B*, the first three samples). Such NR colloids were not detected in strong *CPTL2*-silenced lettuce lines, because of insufficient amounts of NR. Also, GPC-HPLC analysis was unable to detect NR from the noncolloidal, transparent portion, as expected (Fig. 5*C*). Taken together, these results suggest that *CPTL2* silencing causes a significant reduction of NR in lettuce latex, and the corresponding chemical phenotype can be visualized by simple centrifugation. We conclude that *CPTL2* is necessary for NR biosynthesis in lettuce.

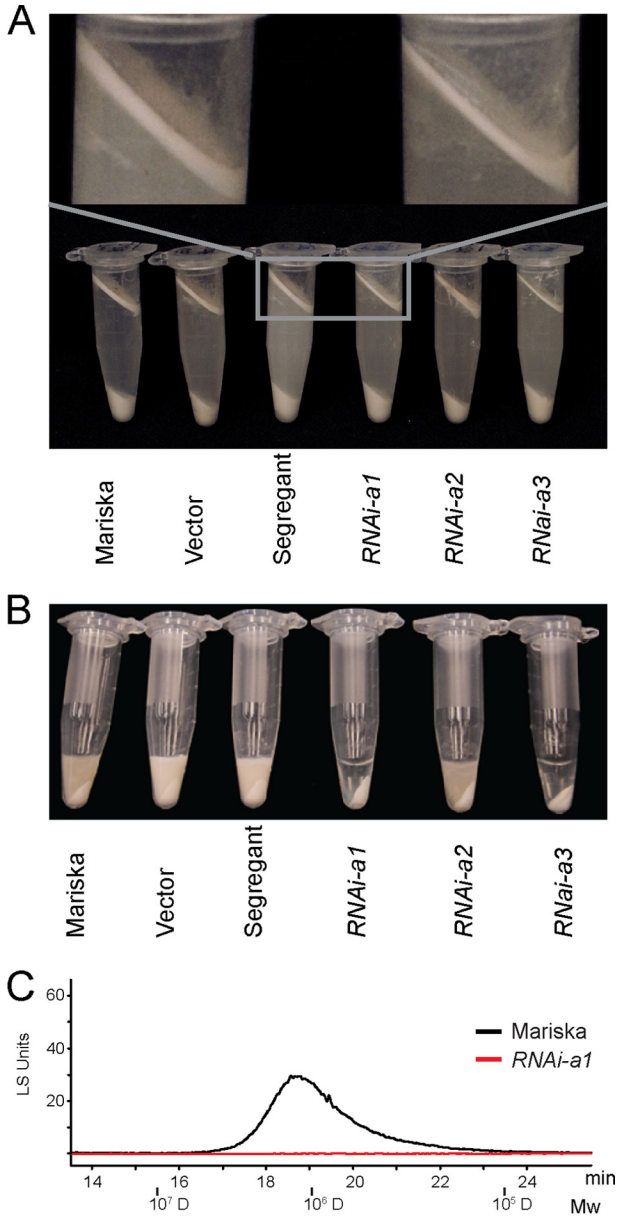

FIGURE 5. **Latex phenotypes from *CPTL2*-silenced lettuces.** *A*, latex layers after centrifugation are shown from *CPTL2*-silenced (RANi-a) and control lettuces (Mariska, vector-transformed, and segregant sibling). 350 mg of latex (fresh weight) was dissolved in 1 ml of extraction buffer as described under "Experimental Procedures." *B*, presence or absence of NR in latex from control or *CPTL2*-silenced lettuces is visualized after SDS addition by centrifugation. *C*, HPLC-GPC analysis of transparent (RNAi-a1) and colloidal (Mariska) portions after centrifugation. 30 mg of latex (fresh weight) was used for each experiment.

Identification of Latex-specific Conventional CPT (CPT3)—During the course of this work, RNAi-mediated silencing of three highly homologous *CPT*s (*TbCPT1-3*; >96% amino acid identity to each other) in dandelion (*Taraxacum brevicorniculatum*) showed the reduction of NR in this plant (20). TbCPTs display very low homology to CPTL2 (17% amino acid identity), and importantly they possess all five conserved motifs required for CPT activity. Thus, these three TbCPTs are conventional CPTs and are clearly distinguishable from the CPTL2-type. Because lettuce and *T. brevicorniculatum* belong to the same subfamily, Cichorioideae, in the Asteraceae family, we exam-

ined the presence of the *TbCPT* ortholog in lettuce. A *TbCPT* ortholog was not identified in the original lettuce transcript data set used for the LC-MS/MS proteomic analysis, which explains the failure of locating a *TbCPT* ortholog from our proteomics data. However, a *TbCPT* ortholog in lettuce, which shares >82% amino acid identity with the TbCPT1-3 proteins, was identified from an updated lettuce transcriptomics data set (updated at NCBI in April 2011 by Dr. Michelmore, UC Davis). This *CPT* was denoted lettuce *CPT3* to distinguish it from the two previously described *CPT*s (lettuce *CPT1/2*). qRT-PCR analysis of *CPT3* in various lettuce tissues showed that *CPT3* expression closely resembled that of *CPTL2*. *CPT3* was exclusively expressed in latex with the highest level of expression in the latex of the flowering stage (Fig. 3*B*).

We questioned whether the abundance of CPT3 protein would be negatively affected in *CPTL2*-silenced lettuce. MRM analysis showed that the relative abundance of CPT3 proteins in RNAi-a1 and RNAi-b1 transgenic lettuce decreased to 31.8 and 46.5% of that in control lettuce, respectively (supplemental Table S2). On the other hand, *CPT3* transcripts in *CPTL2*-silenced lines were not significantly affected (RNAi-a1, 0.83 ± 0.04; RNAi-b1, 1.08 ± 0.08). These data implied that CPT3 protein levels decreased when *CPTL2* is silenced in transgenic lettuce.

Co-localization of CPTL2 and CPT3 on ER in Tobacco—To examine the subcellular localization of CPTL2, GFP was fused to the C terminus of CPTL2, and its localization was examined by confocal microscopy after transient expression in tobacco leaves. CPTL2-GFP was often localized to the perimeters of the round particle, and Nile red dye, known to stain lipophilic substances, stained the core of the round particles labeled by CPTL2-GFP (Fig. 6, *A–C*). Additionally, faint ER signals from CPTL2-GFP were momentarily detected (60–72 h after infiltration; Fig. 6, *D–F*), but this signal rapidly disappeared after 72 h and only round particles were detected. On the other hand, when the *CPT3-GFP* construct was expressed in tobacco leaves, most of the transfected cells showed diffused cytosolic patterns with occasional observations of a blurred ER pattern (Fig. 6, *G–I*). Therefore, by individually expressing *CPTL2* or *CPT3*, their subcellular locations do not entirely overlap with each other.

To allow CPTL2 and CPT3 encounter in the same cells, *CPTL2-GFP* and *CPT3-RFP* (red fluorescent protein) were co-expressed in tobacco epidermis. Surprisingly, CPT3 relocated to ER, resulting in clearly refined ER patterns in both green and red fluorescent channels, and these two signals overlap entirely with each other (Fig. 6, *J–L*). To prove that the GFP signals are associated with ER, untagged *CPTL2* and *CPT3-GFP* were transiently co-expressed with the mCherry-HDEL ER marker. The GFP signals from CPT3-GFP co-localize with the ER marker (Fig. 6, *M–O*).

Subcellular Localization of CPTL2 and CPT3 in Yeast—A yeast strain endogenously expressing *ERG6-RFP* (sterol Δ24 methyltransferase fused with RFP) was used to examine the subcellular localization of CPTL2 and CPT3 in yeast. ERG6 is known to localize to ER/lipid bodies in the log phase and on lipid bodies in the stationary phase. GFP was fused to the C terminus of CPTL2 and CPT3, and these fusion constructs were individually expressed in a yeast strain endogenously expressing *ERG6-RFP* (29). We first examined the yeast cells expressing *CPTL2-GFP* or *CPT3-GFP* during the log phase. When expressed individually, strong CPTL2-GFP was mostly found on the small lipid bodies labeled with ERG6-RFP (Fig. 7, *A–C*). Also, by careful observations, we were able to detect the ER pattern around the nucleus (Fig. 7*A*, *arrows*), although the signals were easy to miss because strong GFP signals from the lipid bodies masked the much weaker ER signals. On the other hand, CPT3-GFP was localized in the cytosol (Fig. 7, *D–F*). By co-expressing *CTPL2* and *CPT3* (one GFP-tagged and the other nontagged), CPT3 relocated, and clear yeast ER pattern was observed for both GFP and RFP channels (Fig. 7, *G–L*). The observed signals on nuclear and periplasmic membranes (nuclear ER and cortical ER, respectively) are typical of ER patterns in yeast (34). The localization data in yeast during the log phase closely mirrored those in tobacco cells.

At the stationary phase, yeast develops larger lipid bodies as shown by an ERG6-RFP marker in Fig. 8. At this stage, CPTL2-GFP was detected in lipid bodies, of which the perimeters were labeled by ERG6-RFP (Fig. 8, *A–C*), but CPT3-GFP showed a diffused pattern in the cytosol (Fig. 8, *D–F*). Such a diffused CPT3-GFP localization pattern was, however, drastically altered by co-expression of nontagged *CPTL2*. Clear relocalization of CPT3-GFP from cytosol to lipid bodies were observed by their co-expression (Fig. 8, *G–I*). In summary, as observed in tobacco cells, the co-expression of *CPTL2* and *CPT3* in yeast facilitates the co-localization of these two proteins on the ER during the log phase and on the lipid bodies in the stationary phase.

Evidence for CPTL2 and CPT3 Interaction by Yeast Two-hybrid Assay—To examine whether the alterations of the localization are the result of the physical interaction between CPTL2 and CPT3, Y2Hs were performed. To mask the putative signal-anchor domain, CPTL2 was fused to the C terminus of the DNA-binding domain (DB) as bait, whereas CPTL2 or CPT3 was fused to the C terminus of the transcription activation (TA) domain as prey. When β-galactosidase assays were performed using the yeast expressing the fusion constructs in all combinations, only yeast expressing *DB-CPTL2* (bait) and *TA-CPT3* (prey) showed reporter enzyme activity (Fig. 9*A*). Only basal level activities of reporter enzyme were detected when yeasts were grown in noninductive glucose medium. When the same experiments were conducted using the reverse orientation (*e.g.* CPT3 as bait and CPTL2 as prey), again only yeast expressing *DB-CPT3* and *TA-CPTL2* showed reporter enzyme activity, although the reporter activity from this combination was 4-fold lower than that from reversed combination (Fig. 9*A*). In addition, the yeast transformants were tested for the ability to grow on amino acid drop-out medium, in which the essential amino acid leucine is absent and only produced when the prey and bait interact. Only yeast containing the DB-CPTL2/TA-CPT3 pair was able to grow (Fig. 9*B*). No growth was observed from the yeast expressing DB-CPT3/TA-CPTL2, perhaps because of their weak interaction in this orientation, as shown in the reporter enzyme assays. These Y2H assay results further support the interaction between CPTL2 and CPT3.

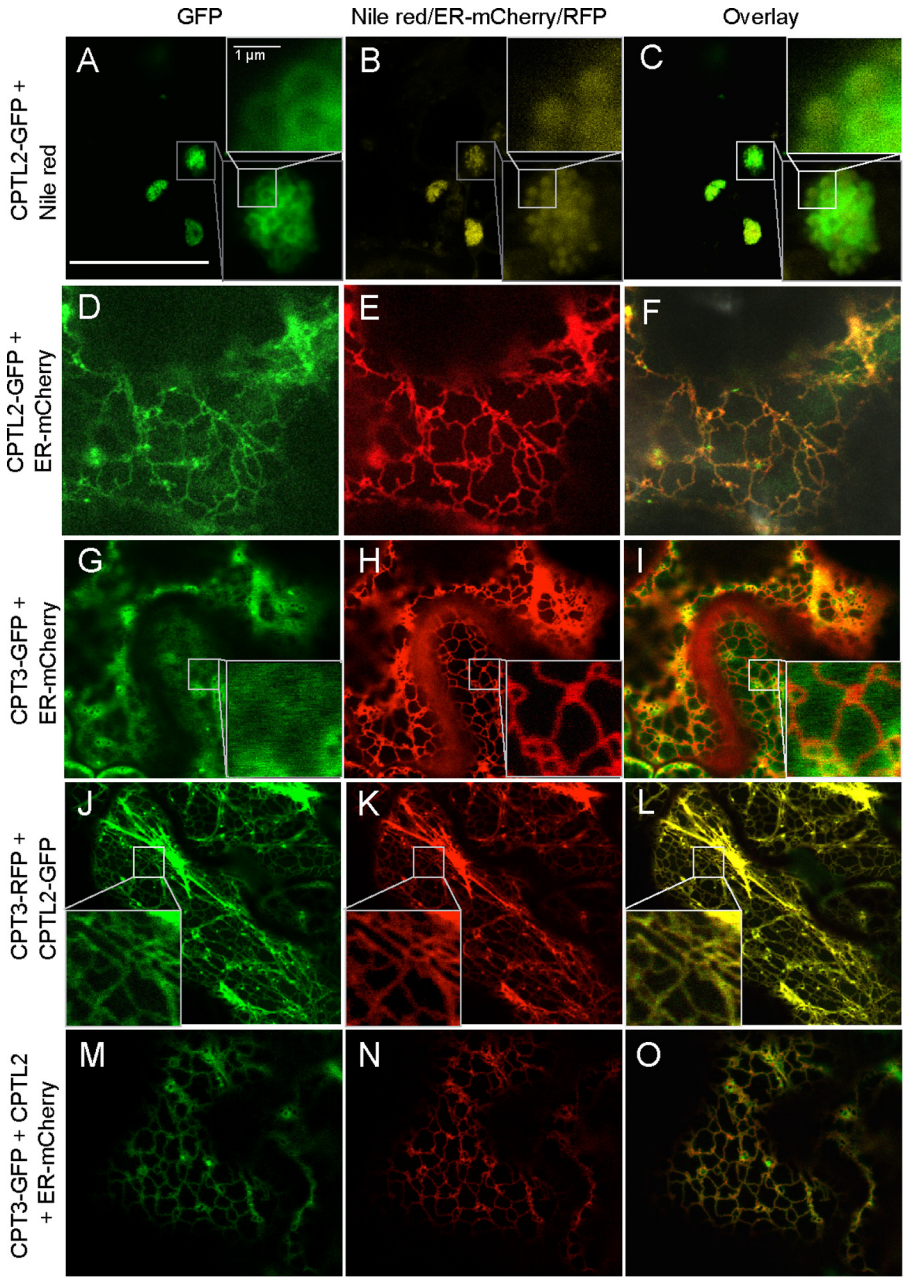

FIGURE 6. **Subcellular localization of CPTL2 and CPT3 in tobacco.** Confocal microscopy was used to capture fluorescent signals from tobacco epidermal cells after transient expression of the various constructs as described below. *A–C*, a single expression of *CPTL2-GFP*; *D–F*, double expression of *CPTL2-GFP* and *mCherry-HDEL*; *G–I*, double expression of *CPT3-GFP* and *mCherry-HDEL*; *J–L*, double expression of *CPTL2-GFP* and *CPT3-RFP*; *M–O*, triple expression of *CPTL2* (untagged), *CPT3-GFP*, and *mCherry-HDEL*. GFP channels are shown in *A*, *D*, *G*, *J*, and *M*; RFP channels are shown in *E*, *H*, *K*, and *N*; Nile red channel is shown in *B*. Images from fluorescent channels were combined in *C*, *F*, *I*, *L*, and *O*. The *bar* in *A* indicates 25 μm.

Biochemical Assays Using CPTL2 and CPT3 Recombinant Enzymes—Catalytic activities of CPTL2 and CPT3 were examined by heterologous expression in *E. coli*. *E. coli*-produced, partially purified CPTL2, CPT3, and their mixture showed no CPT activity *in vitro* (data not shown), whereas the control enzyme, *E. coli* UPPS, prepared using the same method displayed potent activity (44.7 nmol IPP incorporation μg purified protein^{-1} h^{-1}). As an alternative approach, these cDNAs were expressed in the yeast YPH499 strain. FLAG epitope-tagged CPTL2/CPT3, and their respective nontagged versions were generated. In comparison, expression cassettes of an analogous pair, *CPTL1/CPT1*, were also constructed (*CPT2* encodes a chloroplast targeting peptide and thus was excluded from this analysis). These cDNAs were expressed individually or simultaneously in yeast. Immunoblot analyses confirmed the presence of respective recombinant proteins in microsomes and total protein extract (Fig. 10, *A* and *C*). To evaluate the biochemical activities of CPTL/CPT, microsomes containing CPTL/CPT were incubated with ^{14}C-labeled IPPs and FPP, and radioactivities of the chloroform extract from the enzyme reactions were measured and separated by reverse phase TLC (Fig. 10, *B*, *D*, and *E*). In these assays, FLAG-tagged enzymes failed to show ^{14}C-IPP incorporation activity above the vector control activity for both CPTL1/CPT1 and CPTL2/CPT3. However,

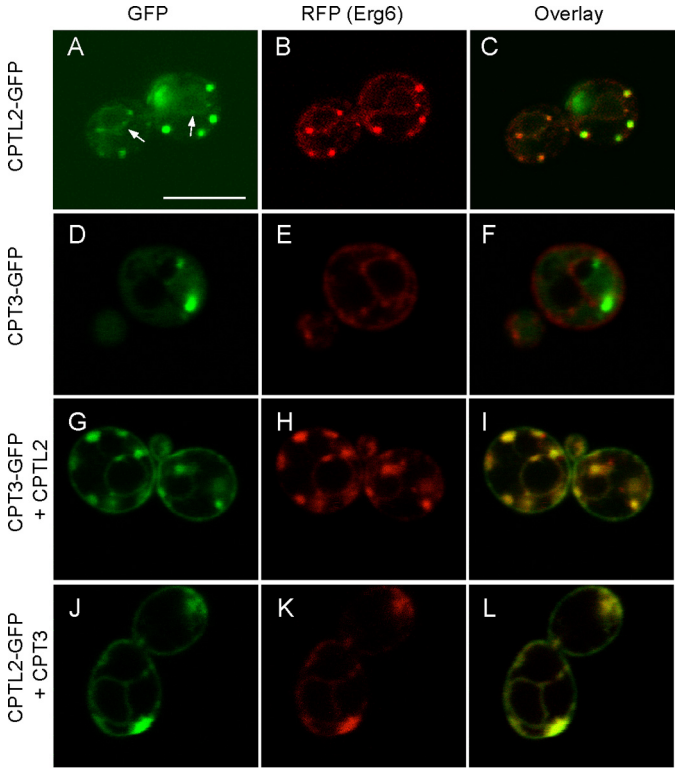

FIGURE 7. **Subcellular localization of CPTL2 and CPT3 in the log phase yeast.** Yeast cells at log phase (8 h after inoculation) were observed by confocal microscopy. *CPTL2-GFP* (*A–C*) or *CPT3-GFP* (*D–F*) was expressed alone in yeast endogenously expressing *ERG6-RFP* (ER and lipid body marker). *Arrows* indicate nuclear ER in *A*. *CPT3-GFP* and untagged *CPTL2* (*G–I*) or *CPTL2-GFP* and untagged *CPT3* (*J–L*) were co-expressed. The *bar* in *A* indicates 5 μm.

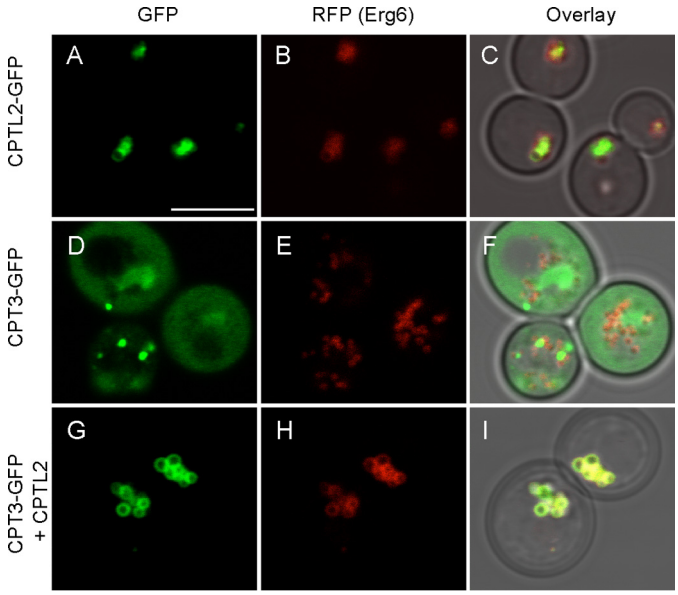

FIGURE 8. **Subcellular localization of CPTL2 and CPT3 in the stationary phase yeast.** Yeast cells at stationary phase (20 h after inoculation) were observed by confocal microscopy. *CPTL2-GFP* (*A–C*) or *CPT3-GFP* (*D–F*) was expressed alone in yeast endogenously expressing *ERG6-RFP*. *CPT3-GFP* and untagged *CPTL2* were co-expressed to examine the change of *CPT3-GFP* localization by *CPTL2* (*G–I*). The *bar* in *A* indicates 5 μm.

when their respective nontagged versions were co-expressed, discernable ^{14}C-IPP incorporated polyisoprene products were observed on TLC in comparison with those from vector control

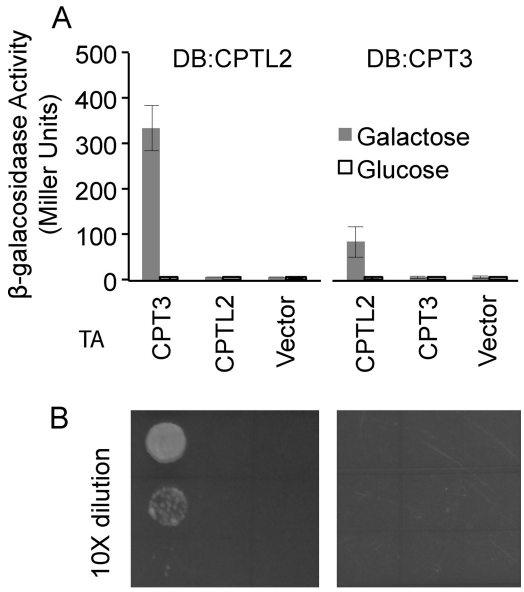

FIGURE 9. **Yeast two-hybrid assays.** *A*, β-galactosidase activity from different combinations of CPTs as bait and prey. The data represent the means ± S.D. from at least three individual transformants. *B*, growth of corresponding yeast on synthetic complete medium lacking leucine.

and FLAG-tagged enzymes (Fig. 10, *B* and *D*). Chloroform extract of the enzyme reactions showed that CPTL1/CPT1 (or CPTL1/CPT1-FLAG) showed a strong IPP incorporation activity (32.9 ± 6.1 pmol IPP h^{-1} μg^{-1} of microsome), which is 13-fold ($n = 3, p < 0.001$) higher activity than the vector control activity (Fig. 10*E*). Although marginal, CPTL2/CPT3 (or CPTL2/CPT3-FLAG) also showed 2.5-fold ($n = 4$, $p < 0.05$) higher IPP incorporation activity (5.9 ± 0.3 pmol IPP h^{-1} μg^{-1} of microsome) than the vector control activity (Fig. 10*E*). Notably, microsomes containing CPTL1/CPT1 incorporated 32% of the total IPP added in the reactions into *cis*-polyisoprenes in 1-h incubation, whereas no ^{14}C-IPP incorporation above the background was detected from CPT1 or CPTL1 alone, even though its protein was detected on microsomes by immunoblot. It should be also noted that only FLAG-tagged CPTL1 or CPTL2 effectively abolished CPT activity, but FLAG-tagged CPT1 or CPT3 had no influence on CPT activity when paired with its corresponding nontagged CPTL (see mix in Fig. 10, *B*, *D*, and *E*), indicating that C-terminal FLAG epitope tag in the CPTL protein blocks CPT activity in the assays. This serendipitous finding provides additional evidence for the interaction and modulation of CPTL on CPT.

We further tested the alternatively paired co-expressions in the enzyme assay (*i.e. CPTL1/CPT3* or *CPTL2/CPT1*). When CPT1 and CPT3 were paired with CPTL2 and CPTL1, respectively, ~70% catalytic activities were obtained in reference to their natural pairs (Fig. 10, *F* and *G*). In particular, efficient dolichol synthesis could be still obtained from the CPT1/CPTL2 pair, implying that both CPTL1 and CPTL2 support the CPT1 dolichol biosynthetic activities. On the other hand, CPT3 activity was still low when it was paired with CPTL1.

As shown in Fig. 8, the CPT relocalization to the lipid bodies in the presence of CPTL is a simple and reliable method to assess the influence of CPTL on CPT localization *in vivo*. We examined whether CPTL1 or CPTL2 can influence the localiza-

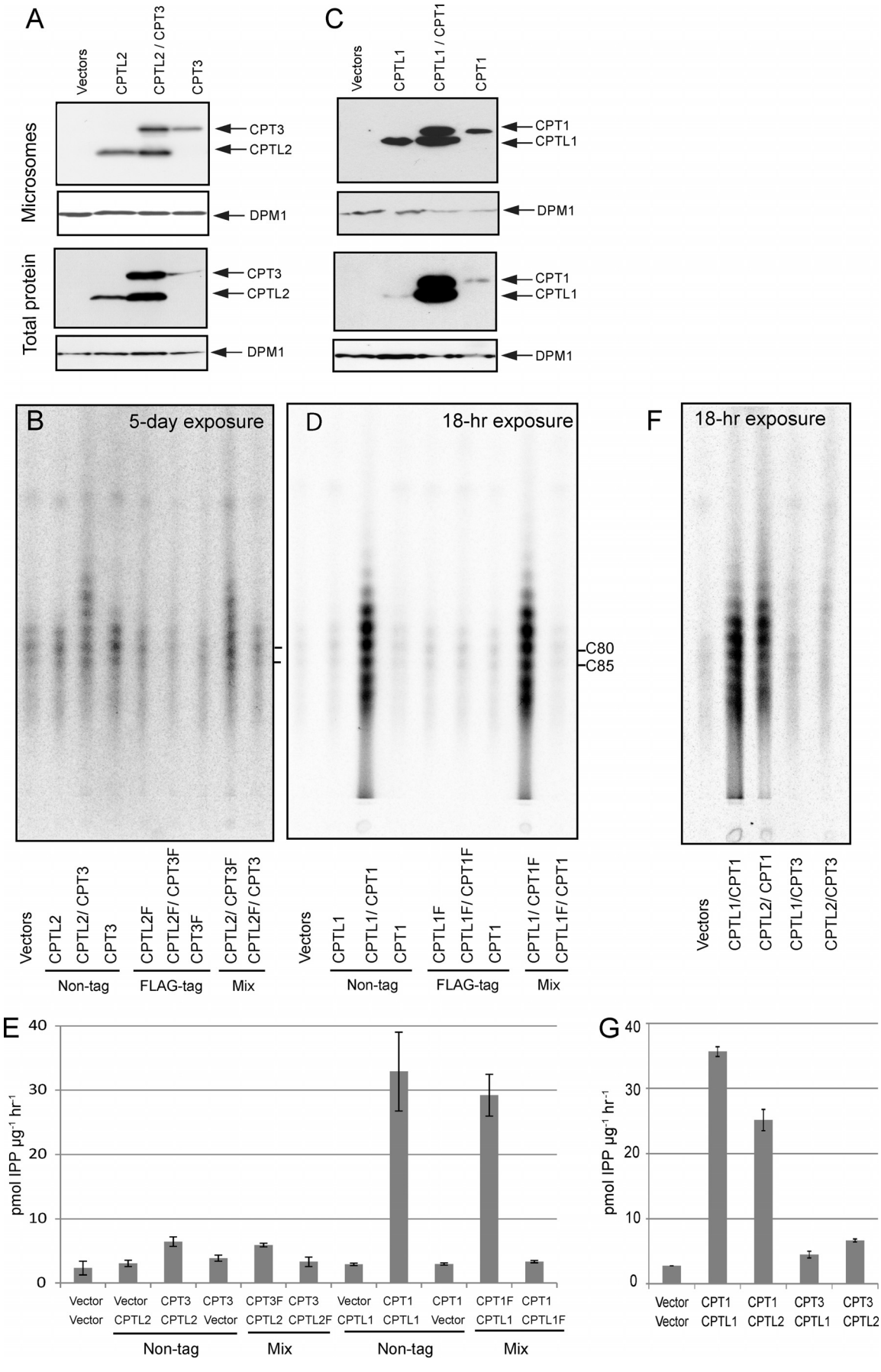
A
Vectors
CPTL2
CPTL2 / CPT3
CPT3
Microsomes
CPT3
CPTL2
DPM1
Total protein
CPT3
CPTL2
DPM1
C
Vectors
CPTL1
CPTL1 / CPT1
CPT1
CPT1
CPTL1
DPM1
CPT1
CPTL1
DPM1
B
5-day exposure
D
18-hr exposure
F
18-hr exposure
C80
C85
Vectors
CPTL2
CPTL2/ CPT3
CPT3
CPTL2F
CPTL2F/ CPT3F
CPT3F
CPTL2/ CPT3F
CPTL2F/ CPT3
Non-tag
FLAG-tag
Mix
Vectors
CPTL1
CPTL1/ CPT1
CPT1
CPTL1F
CPTL1F/ CPT1F
CPT1
CPTL1/ CPT1F
CPTL1F/ CPT1
Non-tag
FLAG-tag
Mix
Vectors
CPTL1/CPT1
CPTL2/ CPT1
CPTL1/CPT3
CPTL2/CPT3
E
pmol IPP µg-1 hr-1
0
10
20
30
40
Vector Vector
Vector CPTL2
CPT3 CPTL2
CPT3 Vector
CPT3F CPTL2
CPT3 CPTL2F
Vector CPTL1
CPT1 CPTL1
CPT1 Vector
CPT1F CPTL1
CPT1 CPTL1F
Non-tag
Mix
Non-tag
Mix
G
pmol IPP µg-1 hr-1
0
10
20
30
40
Vector Vector
CPT1 CPTL1
CPT1 CPTL2
CPT3 CPTL1
CPT3 CPTL2

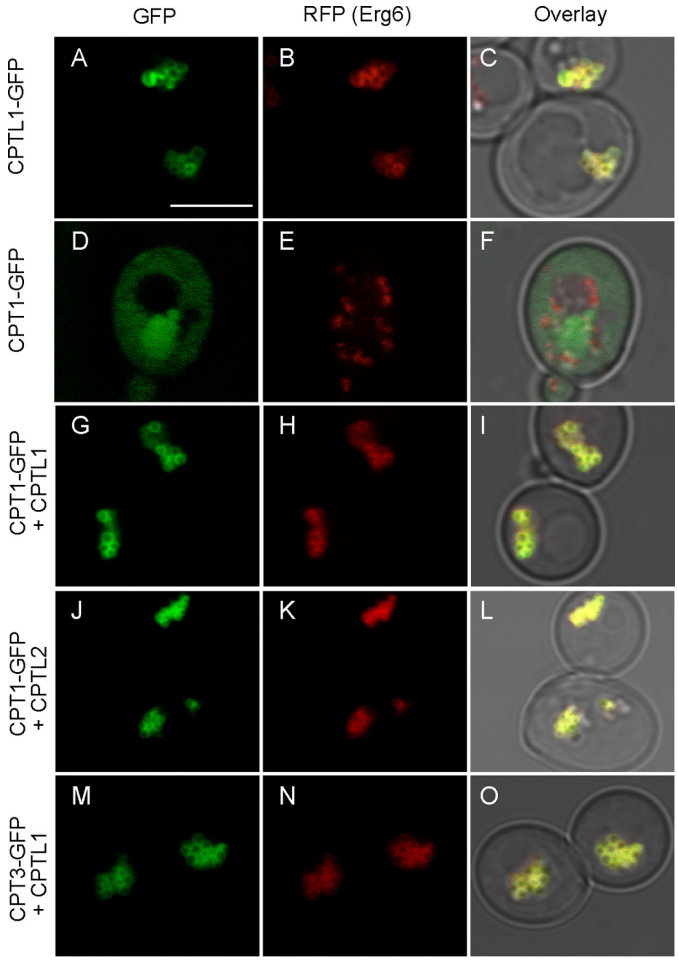

FIGURE 11. **Altered subcellular localization of CPT1 or CPT3 with co-occurrence of CPTL1 or CPTL2 in the stationary phase of yeast.** Yeast cells at stationary phase (20 h after inoculation) were observed by confocal microscopy. *CPTL1-GFP* (*A–C*) or *CPT1-GFP* (*D–F*) was expressed alone in the yeast expressing *ERG6-RFP* (a lipid body marker). CPT1-GFP relocalized to lipid bodies when co-expressed with CPTL1 (*G–I*) or CPTL2 (*J–L*). CPT3-GFP also relocalized to lipid bodies when co-expressed with CPTL1 (*M–O*). *Bar*, 5 μm.

tion of CPT1 or CPT3 by expressing their cDNAs in a pairwise combination. In these experiments, both CPT1 and CPT3 were recruited to the lipid bodies from cytosol, independent of which CPTL was used (Figs. 8 and 11).

In conclusion, efficient *in vitro* synthesis of the dolichol equivalents was demonstrated from the CPTL1/CPT1 assays (Fig. 10*D*), but no evidence of high molecular weight NR synthesis was obtained from the CPTL2/CPT3 assays (Fig. 10*B*). In addition, overall IPP incorporation to polyisoprene was significantly weaker for CPTL2/CPT3 in comparison with CPTL1/CPT1, and the change in CPTL partner did not alter the status of the CPT activity significantly.

DISCUSSION

CPTL2 Is Necessary but Not Sufficient for NR Biosynthesis in Lettuce—NR biosynthesis remains largely unknown in plants. One key finding from this work is that *CPTL2*-silenced lettuce resulted in a dramatic decrease of NR in latex, demonstrating *CPTL2* is necessary for NR biosynthesis. However, purified recombinant CPTL2 from *E. coli* and the microsomes containing CPTL2 from yeast did not show any NR synthetic activity *in vitro*. These data suggest that CPTL2 itself is not sufficient for NR and *cis*-polyisoprene synthesis. It is worth noting that CPTL2 lacks all five conserved motifs of the conventional CPTs (Fig. 2). With such aberrant sequence features in mind, these *in vitro* assay data are not unexpected and are indicative of the nonenzymatic nature of CPTL2 in NR biosynthesis.

Similarly, the most studied CPTL2 homolog, human NgBR, also has no known catalytic activity. Lacking all enzymatic activity, NgBR is able to interact with human CPT (24). Recently, NgBR and its homologs in mice and yeast (NUS1) were identified as necessary subunits for CPT activities in respective organisms (35). NgBR also interacts with Nogo-B and NPC2 for entirely unrelated physiological events, such as remodeling vascular epithelial cells and controlling intracellular trafficking of cholesterol, respectively (23, 25). Therefore, NgBR operates as an ER-residing, multifaceted scaffolding protein in humans. Considering the known NgBR functions and CPTL2 data from this work, we propose that CPTL2 is a scaffolding protein for CPT3 in lettuce.

CPTL homologs in *Arabidopsis* and yeast are *LEW1* and *NUS1* (*YDL193W*), respectively, and their null mutations in each organism are known to be lethal (26, 36). However, no apparent developmental abnormality was observed in the *CPTL2*-silenced lettuce except for NR reduction. This observation indicates that *CPTL2* is not essential for survival but has a specialized role for NR biosynthesis in lettuce latex. On the other hand, the second homologous pair, *CPTL1* and *CPT1*, showed ubiquitous expression patterns in various lettuce tissues (Fig. 3), and the microsomes containing both proteins exhibited an efficient synthesis of short *cis*-polyisoprenes, equivalent to dolichols (Fig. 10*D*). Therefore, the *CPTL1/CPT1* pair is responsible for the biosynthesis of the primary metabolite, dolichols, in lettuce. Lettuce appears to have undergone a gene duplication resulting in the *CPTL1/CPT1* pair for dolichol synthesis in all cells and a specialized *CPTL2/CPT3* pair for NR biosynthesis in latex.

CPTL2 and CPT3 Forms a Protein Complex on ER—A rubber synthase complex has been suggested on rubber particles, yet no tangible experimental evidence has so far been reported. From this work, three lines of evidence support the interaction between CPTL2 and CPT3 to form a protein complex. First, in tobacco epidermis and log phase yeast, we showed that CPT3 relocates from cytosol to ER, when CPTL2 is co-expressed (Fig. 6, *J–L*, and Fig. 7, *G–L*). Second, Y2H assays support direct CPTL2 and CPT3 interaction in yeast. Third, in *CPTL/CPT*-overexpressed yeast, FLAG-tagged CPTL1 or CPTL2 effectively blocked CPT activities, whereas nontagged CPTL1 or CPTL2 allowed CPT activities. These results suggest that C-terminally modified CPTL1/2 can render the CPTL/CPT

FIGURE 10. **CPT enzyme assays and immunoblots using CPT and CPTL recombinant proteins.** *A* and *C*, immunoblots of C-terminal FLAG-tagged CPTL1/2 and CPT1/3 by anti-FLAG antibodies using microsomes and total proteins. The blots were striped and rehybridized with anti-DPM1 (Dol-P-Man synthase) antibodies as controls. *B*, *D*, and *F*, reaction products from the enzyme assays using recombinant CPTL2/CPT3 (*B*), CPTL1/CPT1 (*D*), or alternative parings (*F*) were separated by reverse phase-TLC. *E* and *G*, total activities extracted by chloroform are shown. The data represent the means $\pm$ S.D. ($n \geq 3$).

complex inactive. Collectively, these data indicate that CPTL2 and CPT3 form a hetero-protein complex.

Although the observed protein complex is conceptually new in NR, hetero-protein complexes have been previously reported for enzymes involved in *trans*-isoprenoid biosynthesis. Specifically, to acquire catalytic activities, geranyl diphosphate synthases from three plants (peppermint, snapdragon, and *Clarkia breweri*) (37–39) and heptaprenyl pyrophosphate synthase from *Micrococcus luteus* (40) require heterodimer formations. In these cases, a catalytic TPT subunit needs to form a complex with a noncatalytic subunit that displays overall sequence homology to the catalytic unit. These TPT complexes, composed of a noncatalytic and a catalytic protein, closely resemble the CPTL2 and CPT3 data in this work.

Yeast shows distinct physiological features at a stationary phase, and one of the main changes is the formation of lipid bodies (also called lipid droplets) originating from the ER (41). When nutrition becomes depleted and cell density increases, ER leaflets of the yeast create mono-layered lipid bodies, where triacylglycerols are stored. It is intriguing to observe the localization of the CPTL2-CPT3 complex on lipid bodies during the yeast stationary phase. In many aspects, the rubber particles in the latex of rubber tree resemble lipid bodies in yeast because both have monolayer membranes encapsulating lipophilic substances: triacylglycerol in the lipid bodies and NR in rubber particles (42–44). Their membranes have abundant integral membrane proteins (oleosin in the lipid body and SRPP in the rubber particle) that represent the major components of the membrane proteins. These proteins are known to have structural roles by preventing particle aggregations via charge repulsion (45, 46). Although yeast is a heterologous system for NR metabolism, from the observation of localization of CPTL2/CPT3 on ER in the log phase and on lipid bodies in the stationary phase, this may explain how the ER-synthesized NR is deposited in the rubber particles, analogous to the triacylglycerol deposition in lipid bodies that bud off from the ER (43).

Based on our localization data and the similarities of rubber particles to lipid bodies, we propose a model that CPTL2 anchors CPT3 on ER to form a stable protein complex with its catalytic domain facing cytosol (Fig. 12). It can be inferred from this model that substantial NR could be synthesized on ER, and the monolayer rubber particles filled with NR may bud off from ER. Some residual enzymes and their activities could be transferred to and retained on the rubber particles during rubber particle biogenesis from the ER, therefore accounting for the reported biochemical competency of rubber particles (19). As demonstrated here, the localization of CPTL2 and CPT3 on yeast lipid bodies could offer a convenient experimental system to study NR biosynthesis and storage in yeast. For example, synthesis and accumulation of NR or shorter *cis*-isoprenes in yeast lipid bodies could be traced by feeding radiolabeled mevalonic acid. However, production of NR from the recombinant yeast will be ultimately limited by the low abundance of lipid bodies in yeast, and thus genetically altering the plants that synthesize low quality NR to produce high quality NR is likely to be a more realistic avenue for the high yield NR production, once NR biosynthetic mechanism is fully elucidated.

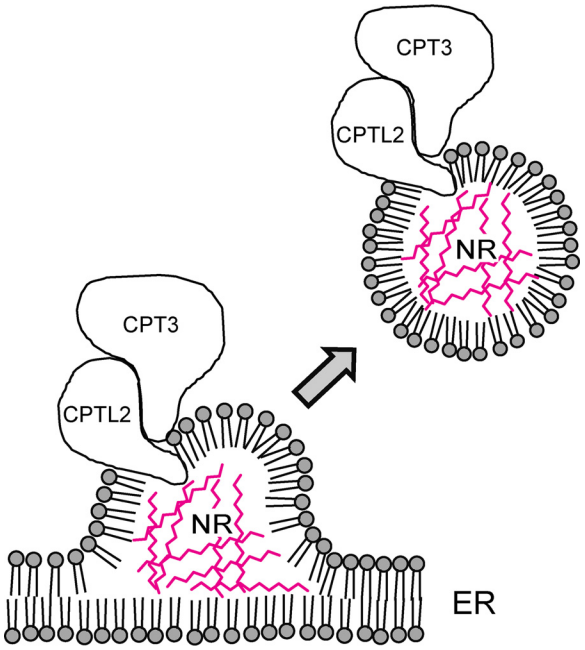

FIGURE 12. **A schematic model of the NR biosynthesis on ER.** This proposed model illustrates the NR biosynthesis on ER from which rubber particles may bud off. CPTL2 resides on ER where it recruits CPT3 to form a stable protein complex. NRs are shown in *red* between the membrane monolayers.

Biochemical Activity of CPTL and CPT—Since the discovery of a prokaryotic CPT, which displays an entirely different sequence and tertiary structure from TPT (5), NR research has focused on identifying distinct *CPT*s from NR-producing species (*e.g.* rubber tree and dandelion) with an aim of synthesizing NR *in vitro*. However, NR biosynthetic activity by purified CPTs has not been reported. In one study, the addition of a latex part to the purified CPT from *E. coli* allowed synthesis of high molecular weight NR (21). However, using yeast recombinant CPT, this NR synthetic activity was not replicated in similar conditions, and only regular dolichols (C80–C100) were produced (22). From dandelion, CPT activity was not directly examined *in vitro* using recombinant CPT but was inferred from the complementation of a *rer2* mutant (16). It is important to note that, to date, all attempts to synthesize NR *in vitro* have centered on conventional *CPT*, and the NR synthetic activity of "conventional CPT together with CPTL" has not been investigated.

In this work, CPT activities from the two pairs of CPTL/CPT (*i.e.* CPTL2/CPT3 and CPTL1/CPT1) were examined as part of microsomes. We found that only the microsomes from the *CPTL/CPT* co-expressed yeast showed *cis*-polyisoprene patterns distinct from the vector control activity (Fig. 10, *B* and *D*). Notably, robust dolichol synthesis was reconstituted *in vitro* using CPTL1/CPT1, but CPTL1 or CPT1 alone did not show activity above the background, despite the presence of these proteins in microsomes. These biochemical data support our proposed role of CPTL1 as a "CPT-scaffolding protein on ER" that can modulate CPT activity, and it becomes apparent that both CPTL1 and CPT1 are required for efficient *cis*-polyisoprene biosynthesis. This finding is further supported by recent CPT activity assays, co-expressing human NgBR/CPT or yeast NUS1/CPT (35). Regrettably, in CPTL2/CPT3 assays, isoprene

polymers larger than the regular dolichols could not be synthesized. Also, the rate of IPP incorporation into dolichols from CPTL2/CPT3 assay was markedly lower than that from CPTL1/CPT1 assay. It is evident that we were not able to synthesize high molecular weight NR by co-expressing *CPTL2* and *CPT3* in yeast. Therefore, present studies showed that CPTL2 is required for NR biosynthesis *in vivo*, but simply blending CPTL2 and CPT3 *in vitro* did not result in NR biosynthesis. Although clear explanation cannot be given from the present data, we speculate that undesirable modifications of CPTL2/CPT3 in yeast could inhibit the NR biosynthetic activity of CPTL2/CPT3 complex, or other latex components may be required to render the CPTL2/CPT3 complex fully active for NR synthesis. Alternatively, a higher dimensional nano-structure, as shown in the cellulose synthase complex (47), could be a prerequisite for NR biosynthesis in plant. Apparently, full *in vitro* synthesis of NR still needs further investigation, and we showed here that lettuce can serve as a powerful system to apply molecular genetics tools to study NR metabolism.

CPTL in the Rubber Tree—We questioned whether the *CPTL* is present in other NR-producing plants and, if so, whether the *CPTL* gene duplication also occurred. In the public database, two *CPTL*s were found in dandelion, which belongs to the same subfamily of lettuce (Chicorioideae), supporting the necessity of a specialized *CPTL* for NR synthesis by a gene duplication (Fig. 2). However, only one member of the *CPTL* was identified in *H. brasiliensis* from 14.3 million transcript reads (Fig. 2). Considering that two copies of *CPTLs* were identified from a relatively small number of transcript reads (<80,000 ESTs) in lettuce and dandelion, insufficient sequencing is not likely the reason for failing to identity the second copy of *CPTL* in the rubber tree. Instead, this analysis suggests that *CPTL* duplication is a recent event in the Chicorioideae subfamily of the Asteraceae family to which both lettuce and dandelion belong. The rubber tree, on the other hand, did not undergo a gene duplication to develop a specialized *CPTL* in latex. Because *CPTL* is clearly required in eukaryotes for *cis*-polyisoprene synthesis (whether it is dolichol or NR) (Ref. 35 and this work), the rubber tree should also require *CPTL* for dolichol and NR biosynthesis. We propose that the single copy of *CPTL* in the rubber tree has a dual role in supporting both the NR synthesis in latex and the ubiquitous dolichol synthesis in other cells. This prediction can be further examined by biochemical and gene expression studies of the rubber tree *CPTL* in the future.

Acknowledgments—We thank Drs. Vanina Zaremberg, Jennifer Cobb, and Marcus Samuel (University of Calgary) for allowing us to use the Erg6-RFP yeast strains, Y2H, and confocal microscope, respectively. Also, we thank Dr. Richard Michelmore (University of California Davis) for supplying us with lettuce seeds, Dr. Brett Phinney (University of California Davis Proteomics Core Facility) for MRM-LC-MS/MS analysis, Dr. David Schriemer (University of Calgary, Southern Alberta Mass Spectrometry Center) for latex proteomics, Dr. Sylvie Jenni (Agriculture Agri-Food Canada) for advising us of lettuce cultivation and crossing techniques, and Dr. Michael Goodin (University of Kentucky) for pSITE vectors.

REFERENCES

1. Cornish, K. (2001) Biochemistry of natural rubber, a vital raw material, emphasizing biosynthetic rate, molecular weight and compartmentalization, in evolutionarily divergent plant species. *Nat. Prod. Rep.* **18,** 182–189
2. Mooibroek, H., and Cornish, K. (2000) Alternative sources of natural rubber. *Appl. Microbiol. Biotechnol.* **53,** 355–365
3. van Beilen, J. B., and Poirier, Y. (2007) Establishment of new crops for the production of natural rubber. *Trends Biotechnol.* **25,** 522–529
4. Tholl, D. (2006) Terpene synthases and the regulation, diversity and biological roles of terpene metabolism. *Curr. Opin. Plant Biol.* **9,** 297–304
5. Fujihashi, M., Zhang, Y. W., Higuchi, Y., Li, X. Y., Koyama, T., and Miki, K. (2001) Crystal structure of *cis*-prenyl chain elongating enzyme, undecaprenyl diphosphate synthase. *Proc. Natl. Acad. Sci. U.S.A.* **98,** 4337–4342
6. Tarshis, L. C., Yan, M., Poulter, C. D., and Sacchettini, J. C. (1994) Crystal structure of recombinant farnesyl diphosphate synthase at 2.6-A resolution. *Biochemistry* **33,** 10871–10877
7. Spiro, R. G. (2002) Protein glycosylation: nature, distribution, enzymatic formation, and disease implications of glycopeptide bonds. *Glycobiology* **12,** 43R–56R
8. Teng, K. H., and Liang, P. H. (2012) Structures, mechanisms and inhibitors of undecaprenyl diphosphate synthase: a *cis*-prenyltransferase for bacterial peptidoglycan biosynthesis. *Bioorg. Chem.* **43,** 51–57
9. Kato, J., Fujisaki, S., Nakajima, K., Nishimura, Y., Sato, M., and Nakano, A. (1999) The *Escherichia coli* homologue of yeast RER2, a key enzyme of dolichol synthesis, is essential for carrier lipid formation in bacterial cell wall synthesis. *J. Bacteriol.* **181,** 2733–2738
10. Sato, M., Fujisaki, S., Sato, K., Nishimura, Y., and Nakano, A. (2001) Yeast *Saccharomyces cerevisiae* has two *cis*-prenyltransferases with different properties and localizations. Implication for their distinct physiological roles in dolichol synthesis. *Genes Cells* **6,** 495–506
11. Sato, M., Sato, K., Nishikawa, S., Hirata, A., Kato, J., and Nakano, A. (1999) The yeast *RER2* gene, identified by endoplasmic reticulum protein localization mutations, encodes *cis*-prenyltransferase, a key enzyme in dolichol synthesis. *Mol. Cell. Biol.* **19,** 471–483
12. Akhtar, T. A., Matsuba, Y., Schauvinhold, I., Yu, G., Lees, H. A., Klein, S. E., and Pichersky, E. (2013) The tomato *cis*-prenyltransferase gene family. *Plant J.* **73,** 640–652
13. Kera, K., Takahashi, S., Sutoh, T., Koyama, T., and Nakayama, T. (2012) Identification and characterization of a *cis,trans*-mixed heptaprenyl diphosphate synthase from *Arabidopsis thaliana*. *FEBS J.* **279,** 3813–3827
14. van Beilen, J. B., and Poirier, Y. (2007) Guayule and Russian dandelion as alternative sources of natural rubber. *Crit. Rev. Biotechnol.* **27,** 217–231
15. Bushman, B. S., Scholte, A. A., Cornish, K., Scott, D. J., Brichta, J. L., Vederas, J. C., Ochoa, O., Michelmore, R. W., Shintani, D. K., and Knapp, S. J. (2006) Identification and comparison of natural rubber from two *Lactuca* species. *Phytochemistry* **67,** 2590–2596
16. Schmidt, T., Lenders, M., Hillebrand, A., van Deenen, N., Munt, O., Reichelt, R., Eisenreich, W., Fischer, R., Prüfer, D., and Gronover, C. S. (2010) Characterization of rubber particles and rubber chain elongation in *Taraxacum koksaghyz*. *BMC Biochem.* **11,** 11
17. Swanson, C. L., Buchanan, R. A., and Otey, F. H. (1979) Molecular weights of natural rubbers from selected temperate zone plants. *J. Appl. Polym. Sci.* **23,** 743–748
18. Seiler, G. J., Carr, M. E., and Bagby, M. O. (1991) Renewable resources from wild sunflowers (*Helianthus spp, Asteraceae*). *Econ. Bot.* **45,** 4–15
19. Cornish, K. (2001) Similarities and differences in rubber biochemistry among plant species. *Phytochemistry* **57,** 1123–1134
20. Post, J., van Deenen, N., Fricke, J., Kowalski, N., Wurbs, D., Schaller, H., Eisenreich, W., Huber, C., Twyman, R. M., Prüfer, D., and Gronover, C. S. (2012) Laticifer-specific *cis*-prenyltransferase silencing affects the rubber, triterpene, and inulin content of *Taraxacum brevicorniculatum*. *Plant Physiol.* **158,** 1406–1417
21. Asawatreratanakul, K., Zhang, Y. W., Wititsuwannakul, D., Wititsuwannakul, R., Takahashi, S., Rattanapittayaporn, A., and Koyama, T. (2003) Molecular cloning, expression and characterization of cDNA encoding *cis*-prenyltransferases from *Hevea brasiliensis*: a key factor participating in natural rubber biosynthesis. *Eur. J. Biochem.* **270,** 4671–4680

22. Takahashi, S., Lee, H. J., Yamashita, S., and Koyama, T. (2012) Characterization of *cis*-prenyltransferases from the rubber producing plant *Hevea brasiliensis* heterologously expressed in yeast and plant cells. *Plant Biotechnol.* **29,** 411–417
23. Miao, R. Q., Gao, Y., Harrison, K. D., Prendergast, J., Acevedo, L. M., Yu, J., Hu, F., Strittmatter, S. M., and Sessa, W. C. (2006) Identification of a receptor necessary for Nogo-B stimulated chemotaxis and morphogenesis of endothelial cells. *Proc. Natl. Acad. Sci. U.S.A.* **103,** 10997–11002
24. Harrison, K. D., Park, E. J., Gao, N., Kuo, A., Rush, J. S., Waechter, C. J., Lehrman, M. A., and Sessa, W. C. (2011) Nogo-B receptor is necessary for cellular dolichol biosynthesis and protein *N*-glycosylation. *EMBO J.* **30,** 2490–2500
25. Harrison, K. D., Miao, R. Q., Fernandez-Hernándo, C., Suárez, Y., Dávalos, A., and Sessa, W. C. (2009) Nogo-B receptor stabilizes Niemann-Pick type C2 protein and regulates intracellular cholesterol trafficking. *Cell Metab.* **10,** 208–218
26. Zhang, H., Ohyama, K., Boudet, J., Chen, Z., Yang, J., Zhang, M., Muranaka, T., Maurel, C., Zhu, J. K., and Gong, Z. (2008) Dolichol biosynthesis and its effects on the unfolded protein response and abiotic stress resistance in *Arabidopsis*. *Plant Cell* **20,** 1879–1898
27. Pfaffl, M. W. (2001) A new mathematical model for relative quantification in real-time RT-PCR. *Nucleic Acids Res.* **29,** e45
28. Zulak, K. G., Khan, M. F., Alcantara, J., Schriemer, D. C., and Facchini, P. J. (2009) Plant defense responses in opium poppy cell cultures revealed by liquid chromatography-tandem mass spectrometry proteomics. *Mol. Cell. Proteomics* **8,** 86–98
29. Huh, W. K., Falvo, J. V., Gerke, L. C., Carroll, A. S., Howson, R. W., Weissman, J. S., and O'Shea, E. K. (2003) Global analysis of protein localization in budding yeast. *Nature* **425,** 686–691
30. Golemis, E. A., Serebriiskii, I., Finley, R. L., Jr., Kolonin, M. G., Gyuris, J., and Brent, R. (2008) Interaction trap/two-hybrid system to identify interacting proteins. *Curr. Protoc. Mol. Biol.* Chapter 20: Unit 20.1
31. Chakrabarty, R., Banerjee, R., Chung, S. M., Farman, M., Citovsky, V., Hogenhout, S. A., Tzfira, T., and Goodin, M. (2007) PSITE vectors for stable integration or transient expression of autofluorescent protein fusions in plants: probing *Nicotiana benthamiana*-virus interactions. *Mol. Plant Microbe Interact.* **20,** 740–750
32. Liang, P. H., Ko, T. P., and Wang, A. H. (2002) Structure, mechanism and function of prenyltransferases. *Eur. J. Biochem.* **269,** 3339–3354
33. Takahashi, S., and Koyama, T. (2006) Structure and function of *cis*-prenyl chain elongating enzymes. *Chem. Rec.* **6,** 194–205
34. Fehrenbacher, K. L., Davis, D., Wu, M., Boldogh, I., and Pon, L. A. (2002) Endoplasmic reticulum dynamics, inheritance, and cytoskeletal interactions in budding yeast. *Mol. Biol. Cell* **13,** 854–865
35. Park, E. J., Grabińska, K. A., Guan, Z., Stránecký, V., Hartmannová, H., Hodaňová, K., Barešová, V., Sovová, J., Jozsef, L., Ondrušková, N., Hansíková, H., Honzík, T., Zeman, J., Hlková, H., Wen, R., Kmoch, S., and Sessa, W. C. (2014) Mutation of Nogo-B receptor, a subunit of *cis*-prenyltransferase, causes a congenital disorder of glycosylation. *Cell Metab.* **20,** 448–457
36. Rabitsch, K. P., Tóth, A., Gálová, M., Schleiffer, A., Schaffner, G., Aigner, E., Rupp, C., Penkner, A. M., Moreno-Borchart, A. C., Primig, M., Esposito, R. E., Klein, F., Knop, M., and Nasmyth, K. (2001) A screen for genes required for meiosis and spore formation based on whole-genome expression. *Curr. Biol.* **11,** 1001–1009
37. Burke, C., and Croteau, R. (2002) Interaction with the small subunit of geranyl diphosphate synthase modifies the chain length specificity of geranylgeranyl diphosphate synthase to produce geranyl diphosphate. *J. Biol. Chem.* **277,** 3141–3149
38. Burke, C. C., Wildung, M. R., and Croteau, R. (1999) Geranyl diphosphate synthase: cloning, expression, and characterization of this prenyltransferase as a heterodimer. *Proc. Natl. Acad. Sci. U.S.A.* **96,** 13062–13067
39. Tholl, D., Kish, C. M., Orlova, I., Sherman, D., Gershenzon, J., Pichersky, E., and Dudareva, N. (2004) Formation of monoterpenes in *Antirrhinum majus* and *Clarkia breweri* flowers involves heterodimeric geranyl diphosphate synthases. *Plant Cell* **16,** 977–992
40. Sasaki, D., Fujihashi, M., Okuyama, N., Kobayashi, Y., Noike, M., Koyama, T., and Miki, K. (2011) Crystal structure of heterodimeric hexaprenyl diphosphate synthase from *Micrococcus luteus* B-P 26 reveals that the small subunit is directly involved in the product chain length regulation. *J. Biol. Chem.* **286,** 3729–3740
41. Wolinski, H., Kolb, D., Hermann, S., Koning, R. I., and Kohlwein, S. D. (2011) A role for seipin in lipid droplet dynamics and inheritance in yeast. *J. Cell Sci.* **124,** 3894–3904
42. Cornish, K., Wood, D. F., and Windle, J. J. (1999) Rubber particles from four different species, examined by transmission electron microscopy and electron-paramagnetic-resonance spin labeling, are found to consist of a homogeneous rubber core enclosed by a contiguous, monolayer biomembrane. *Planta* **210,** 85–96
43. Frandsen, G. I., Mundy, J., and Tzen, J. T. (2001) Oil bodies and their associated proteins, oleosin and caleosin. *Physiol. Plant.* **112,** 301–307
44. Huang, A. H. (1996) Oleosins and oil bodies in seeds and other organs. *Plant Physiol.* **110,** 1055–1061
45. Hillebrand, A., Post, J. J., Wurbs, D., Wahler, D., Lenders, M., Krzyzanek, V., Prüfer, D., and Gronover, C. S. (2012) Down-regulation of small rubber particle protein expression affects integrity of rubber particles and rubber content in *Taraxacum brevicorniculatum*. *PLoS One* **7,** e41874
46. Tzen, J. T., Lie, G. C., and Huang, A. H. (1992) Characterization of the charged components and their topology on the surface of plant seed oil bodies. *J. Biol. Chem.* **267,** 15626–15634
47. Kimura, S., Laosinchai, W., Itoh, T., Cui, X., Linder, C. R., and Brown, R. M., Jr. (1999) Immunogold labeling of rosette terminal cellulose-synthesizing complexes in the vascular plant *Vigna angularis*. *Plant Cell* **11,** 2075–2086